IN VITRO TOXICITY OF ALUMINUM NANOPARTICLES IN HUMAN KERATINOCYTES

THESIS

Stephanie McCormack-Brown, Major, USAF, BSC

AFIT/GIH/ENV/08-M01

DEPARTMENT OF THE AIR FORCE
AIR UNIVERSITY

AIR FORCE INSTITUTE OF TECHNOLOGY

Wright-Patterson Air Force Base, Ohio

AFIT/GIH/ENV/08-M01

IN VITRO TOXICITY OF ALUMINUM NANOPARTICLES IN HUMAN KERATINOCYTES

THESIS

Presented to the Faculty

Department of Systems and Engineering Management

Graduate School of Engineering and Management

Air Force Institute of Technology

Air University

Air Education and Training Command

In Partial Fulfillment of the Requirements for the

Degree of Master of Science in Industrial Hygiene

Stephanie McCormack-Brown, BS, MSA, CIH

Major, USAF, BSC

March 2008

AFIT/GIH/ENV/08-M01

IN VITRO TOXICITY OF ALUMINUM NANOPARTICLES IN HUMAN KERATINOCYTES

Stephanie McCormack-Brown, BS, MSA, CIH
Major, USAF, BSC

Approved:

//signed//	6 Mar 08
Major Jeremy M. Slagley (Chairman)	Date
//signed//	6 Mar 08
Dr. Charles A. Bleckmann (Member)	Date
//signed//	10 Mar 08
Dr. Saber M. Hussain (Member)	Date

Abstract

Nanotechnology promises to be the defining technology of the 21st century. At an annual investment of $1B, it provides significant contributions to manufacturing, medicine, energy conservation, and the environment. Nanoparticles are structures with at least one dimension in the 1 to 100 nanometer (nm) range. DoD and US Air Force interest in aluminum nanoparticles (AL NPs) stems from its ability to enhance combustion jet fuel, thus increasing fuel efficiency. The addition of AL NPs to JP-8 may pose a unique dermal hazard to aircraft maintenance workers. There is no published data on AL NP toxicity effects on human skin. This research used *in vitro* techniques to determine the cytotoxicity of AL NPs, sized 50, 80, and 120 nm, on human keratinocytes. AL NPs at concentrations 10 – 10,000 μg/mL and 24-hour exposure did not have a negative effect on cell viability, as assessed by membrane leakage, metabolic function, and reactive oxygen species generation. Keratinocyte expression of proinflammatory interleukins-1α and -8 was quantified to determine if AL NPs induced precursor cytokines for irritant contact or sensitizer response dermatitis. After 24-hour exposure to AL NPs, keratinocytes expressed significant concentrations of IL-8, 24 – 100 times greater than IL-1α, indicating that AL NPs may induce sensitizer response dermatitis.

Acknowledgments

To Major Jeremy Slagley, my heartfelt appreciation for all the work you did in building the AFIT Industrial Hygiene graduate studies program, for the guidance and patience you showed me throughout this course of study, and for the knowledge and expertise you shared with all your students. To Dr. Saber Hussain, thank you for granting me the opportunity to perform this research and for the instruction you gave me throughout the completion of this work. Thank you for opening your laboratory to AFIT students! To Dr. Charles Bleckman, thank you for your humor and support, and Lt Col David Smith, thank you for your mentorship.

There are many, who without their help, I would never have been able to complete this research. I am indebted to Dr. Laura Braydich-Stolle, Ms. Nikki Schaeblin, Mr. Richard Murdock, and the rest of the AFRL BIN Team; Dr. Amanda Schrand (University of Dayton); Mr. Mike Jubara (ChemSys Inc.); and Captain Brian Clarke.

Finally, a special thank you to my husband for all the extra chores you performed and the hours you dedicated to the girls while I toiled away at homework, projects, and papers. To the girls, without your quiet, and not so quiet, support I would never have completed this thesis or this degree.

Stephanie M. Brown

Table of Contents

Page

List of Figures

Figure Page

List of Tables

List of Abbreviations

1XPBS	One percent phosphate buffered solution
AFRL	United States Air Force Research Lab
AL	Aluminum
AL 50	Aluminum nanoparticles, 50 nanometers
AL 80	Aluminum nanoparticles, 80 nanometers
AL 120	Aluminum nanoparticles, 120 nanometers
AL NP	Aluminum nanoparticle
AL NPs	Aluminum nanoparticle
ATSDR	Agency for Toxic Substances and Disease Registry
BET	Brunauer, Emmett, and Teller
DCHF-DA	2',7'-dichlorohydrofluorecein diacetate
DLS	Dynamic light scattering
DoD	U.S. Department of Defense
ELISA	Enzyme-Linked Immuno Sorbent
FBS	Fetal bovine serum
ICD	Irritant contact dermatitis
IL-1α	Interleukin one alpha
IL-8	Interleukin eight
JP-8	Jet propellant eight
LDH	Lactate dehydrogenase
LPS	Lipoploysacaride
LDV	Laser Doppler velocimetry
MTS	3-(4,5-dimethylthiazol-2-yl)-5-(3-carboxymethoxyphenyl)-2-(4-sulfophenyl)-2H-tetrazolium, inner salt
NASA	National Aeronautics and Space Association
NEHI	Nanotechnology environmental and health implications
NIOSH	National Institute for Occupational Safety and Health
PDI	Polydispersity index
ROS	Reactive Oxygen Species
SRD	Sensitizer response dermatitis
TEM	Transmission electron microscopy
XRD	X-ray powder diffraction

IN VITRO TOXICITY OF ALUMINUM

NANOPARTICLES IN HUMAN KERATINOCYTES

I. Introduction

1.1 Background

"Nanomaterials are a diverse class of small-scale (<100 nm) substances formed by molecular-level engineering to achieve unique mechanical, optical, electrical, and magnetic properties" (Tsuji and others, 2006:42). Commercial and military interest, research, and application of nanotechnology continue to grow, far outpacing studies into its risk to human health and the environment. Department of Defense interest in nanotechnology stems from its application in electronics, munitions, fuels, electrochemical power, and surface coatings. Aluminum nanoparticles (AL NPs) have a role in many of these applications, but there have been few toxicological studies conducted to assess the potential risk to human health.

NASA has proven that the addition of AL NPs to JP-8 produces the same fuel efficiency in pulse detonation engines as non-metallized JP-8, but without the need to add oxygen to the combustion process (Palaszewski and others, 2006:16). The Office of Naval Research and the US Navy Research Laboratory are exploring the use of aluminum nanoparticles in lithium batteries to improve the performance of the polymer electrolytes (Carlin and others, 2006:28). The US Navy is using composites containing aluminum and titanium on high-speed reduction gears sets, installed in 80-ton air conditioning units, to repair rather than replace the worn out gears at an annual savings of $500K (Kabacoff, 2006:41). The US Army is conducting research on the use of AL NPs

in explosives, ammunition, and missile propulsion. Research in nanoscale energetic materials has led to the development of aluminum based metastable intermolecular composites (MIC). MICs are a significant improvement over traditional explosives as the rate of energy released from a MIC reaction can be tailored by manipulating the size of the components (Miziolek, 2006:44).

The addition of AL NPs to JP-8 may pose a new dermal hazard to workers who perform jet engine maintenance and fuel cell repair on aircraft in the US Air Force inventory. Concerns regarding dermal exposure to AL NPs include direct cell toxicity, accumulation in the skin, metabolism of particles into smaller components, or increased particle toxicity after ultra violet irradiation (Tsuji and others, 2006:44).

1.2 Problem Statement

Despite the increased use and manufacture of nanoparticles there is very little toxicology information available regarding the effects of nanoparticles on human skin. The use of AL NPs in electronics, fuel additives, and surface coatings presents a potential occupational hazard to workers in the manufacturing and application of these products. Occupational dermatitis accounts for approximately 20 percent of all occupational illnesses in the United States; therefore, the effect of nanoparticles, specifically aluminum, on human skin requires investigation.

1.3 Research Objectives:

The purpose of this study was to address the following questions in order to evaluate the effects of AL NPs on human keratinocytes.

1. Are AL NPs (50, 80, and 120 nm) toxic to human keratinocytes?
2. Do AL NPs induce reactive oxygen species?

3. Do AL NPs induce an inflammatory response in keratinocytes?

4. Can AL NPs be classified as a skin irritant or sensitizer?

1.4 Research Focus

This study focused on the effects of the *in vitro* exposure of AL NPs, in three sizes and at various concentrations, on human keratinocytes.

1.5 Methodology

In vitro methods were used in this study. Human keratinocytes were cultured in plastic flasks, transferred to cell culture plates, and exposed to various concentrations of AL NPs, in three different sizes (50, 80, and 120 nm) for 24 hours. Cell viability and the proinflammatory response of the keratinocytes were studied.

Cell viability of the keratinocytes, after 24 hours of exposure to various concentrations of AL NPs, was determined by quantifying cell membrane leakage and mitochondrial function through colorimetric techniques. Cell membrane leakage was quantified by measuring the reaction of lactate dehydrogenase and the assay enzyme conversion of resazurin to resorufin (TB306, 2007:2). Cell proliferation was measured by quantifying the conversion of MTS (3-(4,5-dimethylthiazol-2-yl)-5-(3-carboxymethoxyphenyl)-2-(4-sulfophenyl)-2H-tetrazolium, inner salt) to formazan (TB169, 2005:1) by functioning mitochondria. The reactive oxygen species (ROS) concentration was measured, using dischlorodihydrofluorescein diacetate, to determine if ROS were the mechanism that induced cell death.

Keratinocyte proinflammatory response, after 24-hour exposure to various concentrations of AL NPs, was quantified using colorimetric ELISA (Enzyme-Linked

Immuno Sorbent) immunoassays. Colorimetric cytokine kits produced by R & D Systems®, Inc., were used to quantify the proinflammatory cytokines IL-1α and IL-8.

1.6 Assumptions/Limitations

1. The properties of AL NPs may change after dry powder is suspended in keratinocyte exposure media.
2. All keratinocytes dosed with the AL NP suspension were exposed to the same concentration of AL NPs through out the entire incubation period, and that the method of exposure was appropriate
3. Keratinocytes account for 90 percent of the cells in the human epidermis and provide an adequate model for *in vitro* studies.
4. AL NP concentrations used in reactive oxygen species and interleukin experiments were chosen from MTS and LDH assay results, and not based upon particle deposition data.
5. The results of *in vitro* studies may be used to anticipate the results of *in vivo* experimentation.

1.7 Implications

The art and science of industrial hygiene is the anticipation, recognition, evaluation, and control of occupational hazards. As application of nanotechnology has outpaced research of its potential health risks, new occupational hazards may have been introduced into the workplace. This research will help to prioritize further dermal toxicity studies with an aim to developing safe work practices.

1.8 Document Overview

This thesis contains five chapters.

Chapter Two: Provides a literature review of occupational health issues related to nanotechnology, toxicity of elemental aluminum, protective mechanisms of skin, description of dermatitis, and skin cell response to toxic agents.

Chapter Three: Description of methods used to collect data.

Chapter Four: Presentation and analysis of data.

Chapter Five: Explanation of data and identification of further research requirements.

II. Literature Review

2.1 Background

This chapter provides a literature review on the nanotechnology industry, and the heath and safety issues related to this industry. It also includes a description of the human skin, a description of the types of dermatitis, and the cellular response to inflammation. This review shows that toxicity in keratinocytes can be characterized by cell viability and morphology. Current information on the toxicity of elemental aluminum is also included.

2.2 Nanotechnology Industry

Nanotechnology, the development and application of nanoparticles, subassemblies, and nano-based products, promises to exceed the impact of the industrial revolution and is projected to become a $1 trillion market by 2015 (Nel and others, 2006:622). National Science Foundation experts claim that nanotechnology may become the defining technology of the 21st century by driving economic growth, and providing significant contributions to manufacturing, medicine, energy conservation, and the environment (Danoi, 2007:90). Per *The National Nanotechnology Initiative December 2007 Strategic Plan*, the US is committed to "stimulating the discovery and innovation" of nanotechnology. To this end, the President's 2006 budget included over $1 billion for nanotechnology research and development.

2.2.1 Industrial Application on Nanoparticles

"With nanotechnology it is possible to create materials from building blocks the size of atom clusters, which exhibit enhanced electronic, magnetic, optical, and chemical properties…far greater potential than just the inherent 'economy of geometry' of

miniaturization" (Lines, 2008:243). Nanosized particles are structures with at least one dimension in the 1 to 100 nanometer (nm) range. Nanoparticles are either manufactured for commercial use or occur naturally in the environment. The term "ultrafine" is reserved for natural and unintentional nanosized particles. Examples include viruses, particulates formed by forest fires and volcanic eruption, combustion engine by-products, metal fumes, and polymer fumes. Nanoparticle and nanomaterial are terms used to refer to manufactured nanosized powders, fullerenes, buckyballs, and etcetera. The theories of classical and quantum mechanics no longer apply when materials are nanosized and a variety of unexpected properties are possible, to include transparency, hydrophobicity, photoluminescence, toughness and hardness, chemical sensing, and bioavailability (Line, 2008:243). Commercial application of nanoparticles requires such characteristics as small size, narrow size distribution, and low levels of agglomeration.

The current and future applications of nanotechnology include a vast array of industry sectors spanning medicine, plastics, energy, electronics, and aerospace. Due to length of the list, only a few applications and available consumer products are described to provide the reader with an understanding of how the industry is growing.

Bound, nanosized materials are incorporated into consumer products to improve their functionality. The application of nano-thin polymer coatings to automotive glass and sunglasses reduces glare and improves scratch resistance. Hydrophobic, nanosized materials are added to the weave of cotton cloth to create stain resistant, wrinkle-free clothing. Carbon nanotubes are added to materials used to produce sporting equipment, such as bats, golf clubs, and tennis rackets to make them lighter and stronger. Silver nanoparticles are embedded into fabric to produce odor-free, antibacterial clothing

(Maney, 2004). EverClean Technologies, Inc., developed a solution that, when applied to roofs and windows, creates a polymer shield that protects against biological growth and is self cleaning (Danoi, 2007:90). The solution contains titanium dioxide and peroxotitanic oxidizing agents that form a micro-thin crystalline coating when applied to a surface. The titanium dioxide peroxotitanic uses sunlight to decompose organic materials, and the crystal coating reduces surface tension, allowing rain to wash the dirt off the surface. Unbound, nanosized materials are also used in consumer products. Nanosized titanium dioxide is used in sunscreens and cosmetics to increase their ability to block ultra violet radiation. Flex-Power, a pain reliever cream, uses nanosized capsules that contain common, over the counter pain relievers to deliver medicine through the skin (Danoi, 2007:88).

2.2.2 Uses of Aluminum Nanoparticles

Aluminum and aluminum oxide nanoparticles are currently used in scratch- and abrasive-resistant coatings on products such as sunglasses, car finishes, and flooring (Sass, 2007:10).

In October 2006, NASA and the Glenn Research Center published a joint report on the use of metallized gel in jet fuel (JP-8). AL NPs, sizes 60 to 100 nm, were added to JP-8 and combusted in a pulse detonation engine. Research was conducted on JP-8 with an aluminum loading of 4.85 (13.25 grams of AL) to 24.68 (83.58 grams of AL) percent weight. The study proved that an AL NP loading of 12 to 18 percent (by weight) allowed the JP-8 to combust without the addition of oxygen. Adding metallized gel to JP-8 reduces dependence on oxygen for ignition, fuel slosh, leakage, and size of the aircraft (Palaszewski and others, 2006:16).

The Office of Naval Research and the US Navy Research Laboratory are exploring the use of aluminum nanoparticles in lithium batteries to extend the battery life cycles and to improve electrolyte performance (Carlin and others, 2006:28). Lithium alloys are used in high-capacity anodes. However, the alloying metals fragment and lose capacity, reducing the life of the battery. Nanoscale composites containing aluminum undergo reversible lithium alloying over many cycles with minimal loss of capacity (Carlin, 2006:27). AL NPs disrupt the polymer-chain organization and create lithium ion conducting pathways. The US Navy is using composites containing aluminum and titanium on high-speed reduction gears sets, installed in 80-ton air conditioning units, to repair rather than replace the worn out gears at an annual savings of $500K (Kabacoff, 2006:41).

The US Army is conducting research on the use of AL NPs in explosives, ammunition, and missile propulsion. Research in nanoscale energetic materials has led to the development of aluminum based metastable intermolecular composites (MIC). MICs are a significant improvement over traditional explosives as the rate of energy released from a MIC reaction can be tailored by manipulating the size of the components (Miziolek, 2006:44).

2.3 Nanoparticle Health and Safety Issues

The primary heath issue associated with the advent of nanotechnology is the unknown risk the manufacture and use of nanoparticles pose to the worker. Nanosized materials do not exhibit the same characteristics as their macrosized (size > 100 nm) cousins, creating an unknown occupational health risk that is difficult to assess and quantify using traditional industrial hygiene methods and equipment. The health and

safety challenges associated with nanotechnology include (1) the development of instruments that accurately measure the emission of nanoparticles into air and water; (2) development and validation of methods to evaluate the toxicity of nanoparticles; (3) development of models that predict the impact of nanoparticles on human health and the environment; and (4) the creation of robust systems to evaluate and track the health and environmental impact of nanoparticles over their entire cycle (Maynard, 2006:268-269).

2.3.1 Nanoparticle Characteristics

Manufactured nanosized materials pose a unique hazard due to their complex nature (Oberdorster and others, 2005:823). Because the primary characteristic contributing to nanoparticle cytotoxicity is unknown, the following properties must be characterized when conducting cytotoxicity studies: size, shape, state of dispersion, chemical and physical properties, surface area, and surface chemistry.

Proper characterization of nanoparticles used in cytotoxicity studies is required to ensure that the toxicity results are reproducible, and to understand which properties contribute to the biological effects. The size and shape of the nanoparticle influences toxicity by affecting particle deposition in the body, cell inflammation responses, and particle clearance from the body. Nanoparticle dispersion refers to the number of particles that agglomerate versus the number of single particles in the exposure media. Highly disperse particles do not tend to agglomerate and have a greater potential for cellular uptake. Characterization of the chemical and physical properties of the nanoparticles is important, as these properties may be different from the properties of the same material in conventional sizes. Surface area should be measured because as the size of the particles in a given mass of material decreases, the total surface area of the particle

increases, thus a greater proportion of a particle's atoms are available on its surface. An increase in atoms on the surface increases the number of reactions the particle can have with its environment. Finally, surface chemistry must be analyzed as coatings and surface charges may affect how the particle interacts with its environment.

2.3.2 Toxicity of Aluminum by Absorption

The widespread use of aluminum compounds in consumer products such as antacids, astringents, aspirin, food additives, and antiperspirants (ATSDR, 2006) has resulted in a continuous exposure to low concentrations of aluminum. Traditionally, elemental aluminum (Al^{+3}) has not been considered a human ingestion nor dermal hazard. However, in the 1980's, physicians noted that patients undergoing long-term dialysis exhibited aluminum-induced bone and brain diseases caused by the aluminum concentrations found in medications and the water used in dialysis equipment (Alfrey and others, 1980:1509). This suggests that aluminum is toxic to humans once it crosses the epithelium and accumulates in concentrations great enough to induce injury.

The human body does not metabolize aluminum into less hazardous components. Aluminum is removed from the body by healthy kidneys that filter enough aluminum from the blood to minimize its accumulation and toxicity. In people with malfunctioning kidneys, aluminum is a systemic toxin that induces bone and brain diseases. Aluminum accumulation in bone is caused by the disruption of phosphate and calcium absorption, weakening the bone, causing breaks, and forming lesions. The accumulation of aluminum in the brains of dialysis patients produces encephalopathy or "dialysis dementia". Encephalopathy is an irreversible, degenerative brain disease that progresses from speech disorders, to myoclonic jerks, and, finally, to dementia. The average

aluminum concentrations found in the bone and brain tissues of renal-failure patients, who died of dialysis-induced encephalopathy, were eight (bone) and six (brain) times greater than the average concentrations found in people who had died with healthy kidneys (Alfrey and others, 1980:1510). While it is not clear if aluminum is a cause or a result of Alzheimer's disease, aluminum has been found in the brain plaque of Alzheimer's patients. Aluminum is also suspected as a cause of Parkinsonism dementia (Toimela and others, 2006:74). These diseases suggest that if the aluminum concentration in the blood exceeds the kidney filtration capacity, aluminum becomes a systemic toxin in humans.

2.3.3 Toxicity of Aluminum Nanoparticles

Little research has been published on the toxicity of aluminum nanoparticles. The US Air Force Research Laboratory (AFRL) performed cell toxicity studies using AL NPs due to the potential use of these particles in electronics, energetics, and jet fuel. From January 2003 through June 2004, AFRL investigated the cytotoxicity of AL NPs, size 30 nm, on mouse keratinocytes (HEL-30). AFRL performed *in vitro* studies to evaluate mitochondrial function, cell membrane integrity, and cellular morphology of HEL-30 cells exposed for 24 hours to AL NPs at concentrations ranging from 10 to 250 µg/mL. Per their report *In Vitro Toxicity of Nanoparticles in Mouse Keratinocytes and Endothelial Cells*, AL NPs at 30 nm did not induce cell death or changes to the cell.

In the 2005 article, "*In Vitro* Cytotoxicity of Nanoparticles in Mammalian Germ-Line Stem Cells", Braydich-Stolle and others reported that AL NPs, size 30 nm, reduced mitochondrial function and induced cell membrane leakage in mouse spermatogonial stem cells at very low concentrations (less than 10 ug/mL).

In the 2007 article, "Cellular Interaction of Different Forms of Aluminum Nanoparticles in Rat Alveolar Macrophages", Wagner and others investigated the cellular interaction of rat alveolar macrophages with aluminum and aluminum oxide nanoparticles, 24-hour exposure to sizes 30 – 120 nm and concentrations 25 – 250 ug/mL. Macrophage cytotoxicity was determined using *in vitro* methods to evaluate mitochondrial function, cell membrane integrity, and phagocytosis. Wagner reported that aluminum oxide nanoparticles had little to no effect on mitochondrial function, cell membrane integrity, and phagocytosis. However, AL NPs produced a reduction in mitochondrial function (at 100 and 250 μg/mL), no impact on cell membrane integrity, and a decrease in phagocytosis (25 μg/mL). Wagner reported that cytotoxicity became more pronounced as the concentration increased and that the size of the particles did not influence toxicity.

2.4 Occupational Skin Disease

For 2006, the total number of cases of occupational skin diseases was 41,400, accounting for 18 percent of the 228,000 reportable illnesses (US Department of Labor, Jan 2008). The Bureau of Labor Statistics defines skin diseases as "illnesses involving the worker's skin that are caused by work exposure to chemicals, plants or other substances". Examples of occupational skin disease include contact dermatitis, eczema, rashes caused by primary irritants and sensitizers or poisonous plants, oil acne, friction blisters, chrome ulcers, and inflammation of the skin. Aluminum is not designated as an occupational skin hazard; however, aluminum compounds in underarm antiperspirants have been shown to cause rashes (ATSDR, 2006).

2.4.1 Skin Structure

The human skin is comprised of two layers; epidermis is the outer layer and dermis is the inner layer. Comprised of dead keratinocytes and body oil, the stratum corneum is the outer most layer of the epidermis and acts as the body's primary protective barrier. Keratinocytes, melanocytes, Langerhans cells, Merkel cells, and sensory nerves form the epidermis, with keratinocytes accounting for 90 percent of the epidermal layer (see Figure 1). There is a protective barrier at the junction of the two layers. Hair follicles, sebaceous glands, and sweat (apocrine and eccrine) glands residing in the dermis layer may compromise the effectiveness of the protective barrier. The dermis makes up 90 percent of the skin and, through capillaries located at the dermal epidermal junction, supplies blood to the epidermis. Capillaries also supply blood to the hair follicle bulbs and the secretion cells of the eccrine glands. Figure 2 shows the structure of the epidermis and dermis.

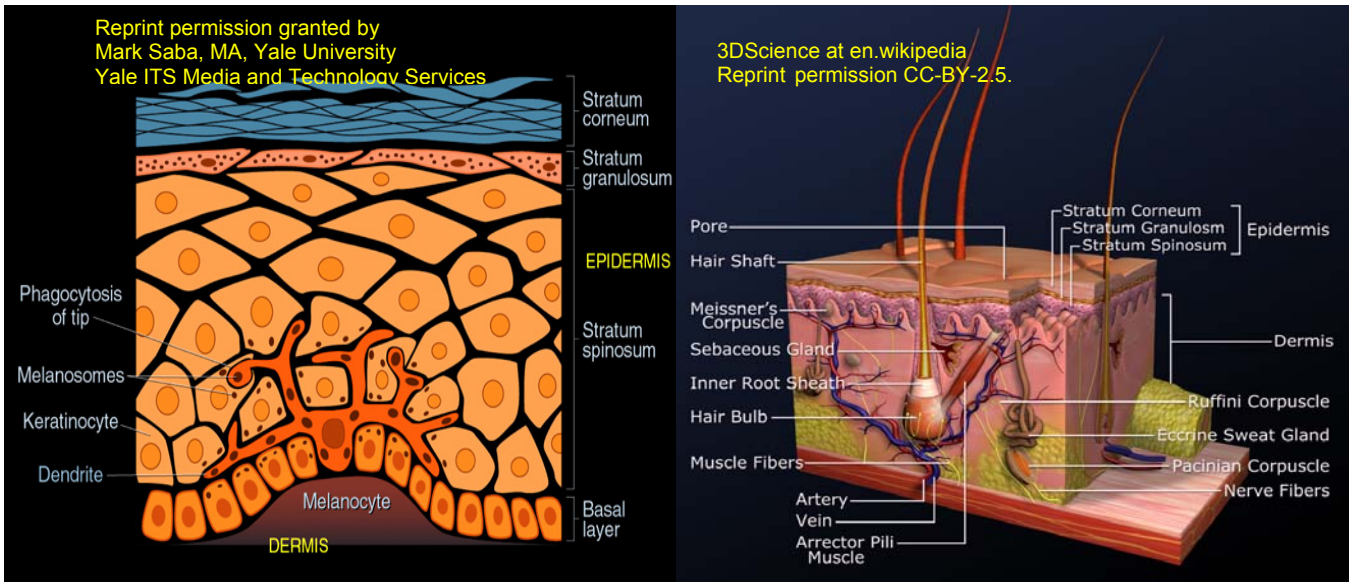

Figure 1 (left). Structure of Epidermis (Mark Saba MA, current as of 10 Jan 07)
Figure 2 (right). Structure of Human Skin (3DScience, 2007)

There are three routes in which foreign materials can enter the body through the skin: material interaction with cells (material uptake or disruption of cellular processes), absorption through spaces between epidermal cells, or penetration through hair follicles and sweat gland orifices. Uncompromised skin cells protect the body by metabolizing materials that cross the stratum corneum before reaching susceptible tissue. Diseases and injuries decrease the ability of the skin to protect the body from absorbing materials through the skin. Fat-soluble chemicals can damage the stratum corneum by dissolving body oils, aiding in the penetration of materials through hair follicles and sweat gland orifices.

2.4.2 Dermatitis

Dermatitis is defined as an inflammation of the skin. Acute skin inflammation can occur from exposure to chemicals or as a response to friction or trauma. The body uses the inflammation process to repair tissue, and to remove foreign material and necrotic cells. Chemical induced inflammation may be caused by contact with a skin irritant, such as an acid or base, or as a immunologic reaction to a sensitizer, such as nickel or latex. Both irritant contact and sensitizer response dermatitis are characterized by itching, redness, and skin lesions (Marzulli and Maibach, 2004:231). At the cellular level, the reaction can be characterized through identification of the types of cytokines secreted by keratinocytes.

2.4.3 Irritant Contact Dermatitis

Irritant contact dermatitis (ICD) can be acute or delayed and occurs as a cellular response to an adequate concentration of a direct-acting cytotoxic agent (Marzulli and Maibach, 2004:231). ICD is a non-immune reaction, limited to the exposed area of the

skin, and is typically reversible. It may occur after a single exposure or after multiple exposures, even if the agent is removed from the skin after each exposure. The extent of the cellular response is dependent on the susceptibility of the exposed individual and the thickness of the skin at the site of exposure (Weltfriend and others, 2004:183).

Once an ICD agent disrupts the skin barrier and damages the epidermis, injured keratinocytes initiate an inflammatory response by releasing proinflammatory cytokines, which are proteins used in cell-to-cell communication (Weltfriend and others, 2004:208). Proinflammatory cytokines include interleukin one alpha (IL-1α) and tumor necrosis factor alpha (TNF-α). TNF-α shares some of the same functions as IL-1α and aids in the activation of immune cells. IL-1α, stimulates endothelial cells and fibroblasts to release mediators that increase the flow of plasma, recruit leukocytes to the injured cells, and initiate cell repair at the site of inflammation (Gregus and Klaassen, 2001:70).

2.4.4 Sensitizer Response Dermatitis

Sensitizer response dermatitis (SRD) may also be acute or delayed and occurs as a cellular response to an adequate concentration of a immunologic cytotoxic agent (Marzulli and Maibach, 2004:231). As with ICD producing agents, the concentration that induces SRD may be reached by a single exposure or by multiple exposures that occur over time. SRD can develop in two ways. The first occurs when a SRD agent disrupts the skin barrier, damages the epidermis, and induces an inflammatory response. In the second, the agent initiates an immunological sensitivity without inducing a dermal reaction.

Sensitization occurs when the SRD agent is carried to the lymph nodes by Langerhans cells, where they interact with T-lymphocytes and produce sensitized T-

lymphocytes (Marzulli and Maibach, 2004:231). The sensitized T-lymphocytes develop an irreversible, immunological memory. This immunological memory will induce a more pronounced inflammation response to subsequent exposures, at the exposure site and, possibly, in other areas of the skin, even when the agent concentration is less than the initial concentration that induced the sensitization.

At the cellular level, SRD agents induce keratinocytes to release proinflammatory cytokines IL-1α, TNF-α, and IL-8. Unlike ICD agents, SRD agents stimulate keratinocytes to release elevated concentrations of IL-8. IL-8 belongs to the family of cytokines called chemokine; cytokines characterized by cysteine residues, expressed by keratinocytes in the presence of IL-1α and TNF-α (Feliciani and others, 1996:306). IL-8 is a chemotactic cytokine that signals neutrophils, white blood cells that kill and digest foreign material, and T-lymphocytes to the cell to begin phagocytosis.

2.4.5 Aluminum Skin Exposure

Although the Occupational Safety and Health Administration (OSHA) does not classify aluminum as an occupational skin hazard, aluminum absorption and skin rashes have been linked to consumer products containing aluminum compounds.

Dermal absorption of aluminum has been reported after application of underarm deodorant (Becaria, 2002:311). Two adult volunteers were dermally exposed to one application of 0.4 mL of 21 percent aluminum chlorate for seven weeks. The results showed that the average AL absorption was 3.6 μg after two weeks. (Flarend and others, 2001:167).

Veine and others investigated three cases of children who were unsuccessfully treated for vaccine-site rashes after they had received vaccines that contained aluminum

hydroxide. Their investigation revealed that all three children also used toothpaste that contained aluminum oxide. When the toothpaste was changed to one that did not contain aluminum, the rashes of all three children responded to treatment within two weeks. Each of the families agreed to resume using the toothpaste containing aluminum oxide. In two cases, the child's rash returned within four days. Veine and others concluded that aluminum is a mild, but rare allergen.

2.4.6 Nanoparticle Skin Exposure

Concerns regarding dermal exposure to nanoparticles include direct cell toxicity, accumulation in the skin, metabolism of particles into smaller components, or increased particle toxicity after ultra violet irradiation (Tsuji and others, 2006:44). Permanent accumulations of nanosized silica have been found in the dermis of the feet of patients with Elephantiasis, a condition caused by parasitic obstructions in the lymphatic system of the lower legs (Hoet and others, 2004:9). Toxicologists have shown that 1 μm fluorescent beads can migrate through flexed and broken epidermis where they accumulate in the dermis layer (Oberdorster and others, 2005:834).

2.5 Cell Viability

In vitro analysis of necrosis and cell proliferation is used to determine the viability of cells after exposure to an agent. The source of cell death determines which path the process will follow until the result is necrosis or apoptosis.

Apoptosis or programmed cell death is a "controlled physiologic process of removing individual components of an organism without destruction or damage to the organism" (Fink and Cookson, 2005:1908). Apoptosis occurs in the normal turnover of healthy tissue or from exposure to a cytotoxic agent. Cells contain caspases, enzymes

that when activated, initiate apoptosis. During apoptosis, the cell partitions DNA, cytoplasm, intact mitochondria, and other organelles into bundles bound by a membrane (Wyllie, 2008:3). *In vivo,* the bundles are phagocytized by macrophages and inflammation does not occur. The bundles may swell and leak during *in vitro* experiments where macrophages are absent, causing secondary necrosis and the mitochondria in the bundles remain functional (Wyllie, 2008:3). Autophagy occurs *in vivo* when apoptotic bundles and cellular debris is phagoytized by macrophages and neighboring cells. Pyroptosis is the form of cell death that occurs when the cell is invaded by an infectious agent.

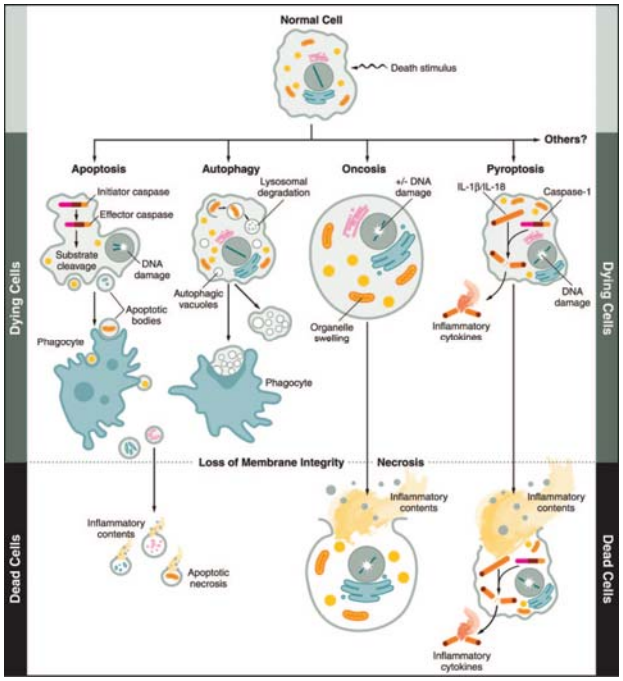

Figure 3. Pathways of Cell Death. Copyright by American Society for Microbiology, published by Fink and Cookson, 2005:1909.

2.5.1 Necrosis

Necrosis describes non-apoptic, accidental cell death, with an uncontrolled release of cell material that may induce inflammation in the surrounding tissue (Fink and

Cookson, 2005:1910). Cytotoxic agents, such as bacteria, viruses, and chemicals can induce cell membrane leakage. Cell membrane damage can be caused by direct contact with the agent or from damage to cellular DNA. Oncosis is the cell death pathway that occurs when cellular DNA is damaged. The repair of cellular DNA begins a cascade of events that damage the cell's ability to maintain homeostasis. As the cell works to repair its DNA, it increases is energy consumption that depletes its energy stores. This uncontrolled use of its energy stores causes the cell to die. As the cell dies, the integrity of its membrane is compromised, and the ion pumps that maintain ion balance within the cytoplasm fails. The imbalance of ions causes the cell to swell and rupture, or cytoplasm to leak through the membrane. Release of the cytoplasm and its contents may cause inflammation in the surrounding tissue.

Lactate dehydrogenase (LDH) is contained in the cytoplasm of eukaryotic cells; therefore, cell membrane leakage can be quantified by measuring the colorimetric reaction of LDH with an assay enzyme that converts a dye, resazurin, to resorufin (TB306, 2007:2). The concentration of LDH is inversely proportional to the number of living cells.

2.5.2 Cell Proliferation

In eukaryotic cells, mitochondria are essential to cell activity. Reduced mitochondrial function indicates that a cell is not proliferating. Reduced cell proliferation may be the result of apoptosis, autophagy, oncosis, or pyroptosis. Mitochondria in healthy, living cells convert MTS (3-(4,5-dimethylthiazol-2-yl)-5-(3-carboxymethoxyphenyl)-2-(4-sulfophenyl)-2H-tetrazolium, inner salt) to formazan

(TB169, 2005:1). Therefore, the concentration of formazan is directly proportional to the number of living cells.

2.5.3 Reactive Oxygen Species

The formation of reactive oxygen species (ROS) and the release of metal ions are the two main mechanisms by which nanoparticles cause cell death (Maysinger and others, 2006:12).

Reactive oxygen species in the form of hydrogen peroxide and superoxide radicals are the result of normal cellular processes. They are generated by electrons that leak from enzymes used in the mitochondria electron transport chain (Becaria and others, 2002:314) and by the cell's metabolic processes. Oxidative stress occurs when the concentration of the ROS exceeds the cell's antioxidant defenses (Xia and others, 2006:1795). Cell damage occurs when the ROS are converted to hydroxyl radicals, which can cause cell necrosis or induce apoptosis by damaging cell DNA, cell organelles, or cell membranes. The cell damage caused by the ROS may induce inflammation in surrounding tissue.

Nanoparticle induced ROS are created when electrons transfer from the nanoparticle to the cell's oxygen molecules or when metal ions disrupt the cell's oxidation/reduction (redox) signaling. Fluorescent probes are used in *in vitro* studies to identify the species and quantify the concentration of the ROS. The fluorescent probe, dischlorodihydrofluorescein diacetate, is used to perform initial ROS screening as it can detect and aid in quantifying all forms of ROS (Maysinger and others, 2006:13).

2.6 Interleukin Expression

"The ability to accurately predict the skin irritating and/or sensitizing potential of newly synthesized chemicals remains a key element in assessing the safety of those products" (Coquette and others, 1999:868). If a chemical migrates through the stratum corneum and reaches the living cells in the epidermis, it may damage the integrity of the keratinocyte membrane, and induce cellular production and/or release of proinflammatory cytokines. Proinflammatory cytokines are key signaling agents that lead to *in vivo* skin irritation or sensitization. As a result, human keratinocyte expression of these cytokines may be an effective screening model for classifying agents as irritants or as sensitizers.

IL-1α is synthesized by the mitochondria (Coquette and others, 1999:875) and IL-8 is synthesized when the nuclear factor-kappa beta is activated by protein kinase C (Chabot-Fletcher and others, 1994:509). IL-1α initiates the inflammation process when released from the cells. IL-1α may be released when the cell membrane is compromised or when the cell is stimulated. In addition to starting the inflammation process, IL-1α stimulates the release of secondary mediators, including IL-8. IL-8 is a chemotactic cytokine that signals neutrophils and T-lymphocytes to the cell to begin phagocytosis.

Coquette and others performed *in vitro* studies of cytokine expression by human keratinocytes exposed to chemicals known to induce ICD and SRD. The study included quantification of intercellular and extracellular IL-1α and IL-8 concentrations, and the assessment of cell viability by MTT, 3-(4,5-dimethylthiazol-2-yl)-2,5-diphenyltetrazolium bromide. MTT is an alternative to MTS and evaluates cell viability in the similar manner as MTS. In their research, Coquette and others quantified the

extracellular concentrations of IL-1α and IL-8 using Quantikine® immunoassay kits (R & D Systems® Inc., Abingdon, UK). The results of their 2003 study showed that keratinocytes expressed both IL-1α and IL-8 when dosed, for 20-hours, with either an irritant or a sensitizer at concentrations ranging from 125 to 4000 μg/mL. They reported that IL-8 expression by keratinocytes exposed to irritants was very low. In contrast, irritants induced expression of high levels of IL-1α. Keratinocytes dosed with sensitizers produced the inverse cytokine profile, high IL-8 and low IL-1α expression. For irritants, they found that as cell death increased (reduced MTT results), the released concentration of IL-1α increased. For sensitizers, there was no correlation between the concentrations of released IL-1α and IL-8, and cell viability. They also reported that the ratio of IL-8 to IL-1α concentrations for irritants ranged from 0.2 to 0.7 (extracellular) and 0.1 to 0.3 (intracellular), and for sensitizers 8.4 to 41.0 (extracellular) and 1.3 to 7.1 (intracellular). Coquette and others concluded that the assessment of cell viability coupled with the measurement of IL-1α and IL-8 expression is a potential *in vitro* method for classifying irritant and sensitizer agents.

III. Methodology

3.1 Introduction

The goal of this study was to determine if AL NPs induced cell death, generated reactive oxygen species, and inflammation in human keratinocytes. Included in this research was the characterization of AL NPs suspended in keratinocyte (HaCaT) exposure media. All research was performed using *in vitro* methods. Before each experiment, cells were prepared in two steps. In the first step, cells were seeded and grown for 24 hours. The second step consisted of exposing the cells to AL NPs, at various concentrations, for 24 hours. This section describes the assumptions, laboratory equipment, nanoparticles, and the experiments used to gather the data.

3.2 Assumptions

Several assumptions were made at the beginning of this study.

1. The properties of AL NPs may change after dry powder is suspended in keratinocyte exposure media.
2. All keratinocytes dosed with the AL NP suspension were exposed to the same concentration of AL NPs through out the entire incubation period, and that the method of exposure was appropriate
3. Keratinocytes account for 90 percent of the cells in the human epidermis and provide an adequate model for *in vitro* studies.
4. AL NP concentrations used in reactive oxygen species and interleukin experiments were chosen from MTS and LDH assay results, and not based upon particle deposition data.
5. The results of *in vitro* studies may be used to anticipate the results of *in vivo*

experimentation.

3.3 Cell Line

The HaCaT cell line consists of immortalized adult human keratinocytes developed by the German Cancer Research Center (DKFZ, Heidelberg, Germany). HaCaT keratinocytes do not produce tumors when passaged/grown indefinitely. When transplanted onto nude mice, HaCaT keratinocytes differentiate into epidermal tissue by forming squame cells and stratifying into epidermal layers (Boukamp and others 1998:761 and 770). Immortalized keratinocytes may be grown indefinitely in cell media without changes to morphology and replication rate. HaCaT keratinocytes behave like normal keratinocytes in terms of growth and differentiation, therefore, this cell line is a suitable *in vitro* model for dermal cytotoxicity studies. This cell line does not include Langerhans cells, which play an important role in the study of immune response and cytokine production.

3.4 Cell Culture

Cells were grown in RPMI-1640 cell media containing HEPES (4-(2-hydroxyethyl)-1-piperazineethanesulfonic acid), sodium pyruvate, L-glutamine, glucose, and bicarbonate (purchased from ATCC®, Manassas VA), and supplemented with 10 percent fetal bovine serum (FBS). To prevent bacterial growth, one percent of penicillin/streptomycin solution (Sigma-Aldrich Chemical Company, St. Louis, MO) was added to the cell growth media. Exposure media (growth media minus the FBS) was used during nanoparticle dosing to maintain cell viability while discouraging cell proliferation. In the ROS experiments, the RPMI-1640 in the cell growth and exposure media was replaced with F-12 Ham with Kaighn's modification (Ham's F-12K) media

(Sigma-Aldrich Chemical Company, St. Louis, MO). Ham's F-12K did not contain phenol red, which interferes with ROS measurement. For morphology and assay experiments, the cells were seeded in 6- or 96-well plates at concentrations ranging from 50K to 300K cells per well. Keratinocytes were grown in a humidified incubator at 37°C ± 0.3°C and 3-5 percent CO_2 atmosphere. For instructions used for cell maintenance, see Appendix A.

3.5 Cell Count and Plating

An adequate number of cells per mL were required in order to perform accurate assay experiments. Cell counting was performed by pipetting 10 µL of high concentration cell suspension on to a hemocytometer. The cells located on each corner grid were counted. The average number of cells per 10 µL was converted to cells per mL. See Appendix B for detailed instructions.

3.6 Nanoparticles

The nanoparticles (NovaCentrix™ Inc., Austin, TX) used in these experiments were aluminum with diameters of 50, 80, and 120 nm. These nanoparticles were originally obtained in 2005. Each sized AL NP, in powder form, was weighed and added to HaCaT exposure media to create stock solutions of 1 mg/mL and 10 mg/mL. Before cell dosing, each stock solution was sonicated for approximately 20 seconds to reduce particle agglomeration. Cell dosing concentrations were calculated based on the required total volume (dosing and exposure media) for either the 6- or the 96- well plates. For example, in a 96-well plate the addition of 20 µL (to each well) of 10 mg/mL dosing stock and 180 µL (to each well) of HaCaT exposure media produced a 1000 µg/mL AL NP dose to the cells in the well. In the ROS experiments, the AL NP dosing stock

solution was made in the same manner as the dosing stocks used throughout the rest of this study, except that Ham's F-12K exposure media was used in place of RPMI-1640.

3.7 SpectraMax®190 and Gemini XPS

The spectrometers, SpectraMax 190® and Gemini XPS (Molecular Devices™ Inc., Sunnyvale, CA) microplate readers, were used to measure light absorbance or emission, respectively, for data quantification in LDH, MTS, ROS, and interleukin assay experiments. SOFTmax® Pro (Molecular Devices™ Inc., Sunnyvale, CA) software was used to run the spectrometers and present the data electronically.

3.8 LDH Assay

The LDH assay was used to determine cell membrane integrity after AL NP exposure. A 96-well plate was seeded with 50K keratinocytes per well and incubated for 24 hours. The growth media was then removed and the cells were dosed with AL NP stock (four wells per concentration per nanoparticle size) and exposure media. For the experiment (zero) control wells, the growth media was removed and 200 μL of exposure media was added. The plate was placed in the incubator. After 24 hours, the plate was removed from the incubator. Being careful not to pipette the nanoparticles, 50 μL of supernate was transferred from each well to a clean 96-well plate, and the LDH assay experiment was performed. See Appendix C for experiment procedures. Each LDH experiment was completed in triplicate. Membrane integrity was assessed for cells exposed to AL NP concentrations ranging from 10 to 10,000 μg/mL.

3.9 MTS Assay

The MTS assay was used to determine the effects of AL NPs on cell growth/proliferation. A 96-well plate was seeded with 50K keratinocytes per well and

incubated for 24 hours. The growth media was then removed and the cells were dosed with AL NP stock (four wells per concentration per nanoparticle size) and exposure media. For experiment control wells, the growth media was removed and 200 μL of exposure media was added. The plate was placed in the incubator. After 24 hours, the plate was removed from the incubator, the cell supernate was removed, and each well was rinsed three times with one percent phosphate buffered solution (1X PBS). HaCaT exposure media and MTS reagent were added to each well, and the plate was incubated for four hours. When the centrifuge was available, the plate was placed in a centrifuge for six minutes, and 100 μL was transferred from each well to a clean plate. When the centrifuge was not available, 100 μL was transferred from each well to a clean plate. These steps were performed to ensure that any remaining AL NPs would not cause false results. See Appendix D for experiment procedures. Each MTS experiment was performed in triplicate. Cell proliferation was assessed for cells exposed to AL NP concentrations ranging from 10 to 10,000 μg/mL.

MTS results at AL NP concentrations greater than 2000 μg/mL were greater than the zero control, which suggested that there might be nanoparticle interference. A second MTS experiment was performed, in triplicate, for 0, 2000, 4000, 6000, 8000, and 10,000 μg/mL and sizes 50, 80, and 120 nm. Spectrofluorometer readings were taken after rinse, but before plates were placed in the centrifuge, after the plates were placed in the centrifuge for six minutes, and after centrifuge and transfer of 100 μL to a clean plate.

3.10 Reactive Oxygen Species

Oxidative stress of keratinocytes exposed to AL NPs was evaluated by measuring the fold-increase of the ROS produced by the cells. Keratinocytes were grown in a 96-

well plate for 24 hours. Before dosing with AL NPs, a fluorescent probe was applied under light controlled conditions. After dosing cells with AL NPs (concentrations 10, 100, 500, 1000, and 2000 μg/mL for sizes 50, 80 and 120 nm), the ROS was measured at zero, one, two, four, six, and twenty-four hours. Each experiment was performed in triplicate. For details on the ROS experiment procedures, see Appendix E.

3.11 Cell Morphology Experiment

A cell morphology experiment was performed on keratinocytes exposed to AL NPs and talcum powder at concentrations ranging from 2000 to 10,000 μg/mL to determine if the nanoparticles or media turbidity caused reduced mitochondrial activity. Talcum powder was chosen for this experiment because it is neither nanosized nor cytotoxic.

Keratinocytes were seeded at a density of 300K cells per well onto four 6-well plates and grown until cells were 100 percent confluent (24-hours). After the growth media was removed from all plates, one well from each of the three plates was dosed with AL NPs at concentrations of 0, 2000, 4000, 6000, 8000, or 10,000 μg/mL (for each nanoparticle size. At the same concentrations, talcum powder dosing stock was added to each well of the fourth plate. After incubation for 24 hours, the dosing stock was removed, and each well was rinsed three times with 1XPBS. Change in cell growth was studied using an Olympus® 1x71 inverted microscope (Olympus® Corp, Tokyo, Japan) equipped with a Retiga 4000R (QImaging® Inc., Surrey BC, Canada) camera and QCapture Pro™ (QImaging® Inc., Surrey BC, Canada) software.

The pH of the AL NP dosing stock, talcum powder dosing stock, and cell supernate (after 24-hour exposure) was measured to determine if pH might be responsible

for cell death at dosing concentrations greater than 2000 ug/mL. Four 6-well plates were seeded and dosed in the same manner as the cell morphology experiment. Before dosing the keratinocytes, the pH of the AL NP and talcum stocks were measured with pH strips (Whatman® pH Indicator Strips, Whatman® Inc., Florham Park, NJ). After 24 hours of exposure to the dosing stock, the pH of each well was measured.

3.12 Interleukin Assays

Human keratinocyte external expression of IL-1α and IL-8, after 24 hour exposure to AL NPs at concentrations 0, 10, 100, 1000, and 2000 μg/mL, was quantified using Quantikine® immunoassay kits (R & D Systems® Inc., Minneapolis, MN). Keratinocytes were seeded, at 300K cells per well, onto three 6-well plates. After 24 hours of incubation, the HaCaT growth media was removed from the wells, the cells were dosed with AL NPs, exposure media, and 125 μl of LPS (final concentration of 25 ug/mL per well), and returned to the incubator for 24 hours. LPS is a component of the outer membrane of gram-negative bacteria and is used to stimulate cells during *in vitro* studies. Two zero controls were used, one with LPS and one without LPS. After the second incubation, the cell supernate was transferred from each well to sterile, 15 mL conical tubes. To minimize AL NP interference, the conical tubes were placed in a centrifuge for 15 minutes at 1200 RPM. To minimize bias, both zero controls were placed in the centrifuge. To ensure that interleukins remained in suspension, each conical tube was placed on a vortex mixer for 15 seconds before transfer to the assay 96-well plate. See Appendices F and G for experiment procedures.

3.13 Aluminum Nanoparticle Characterization

Characterization of size, dispersion, and chemical and physical properties of AL NPs suspended in solution, and the surface chemistry of nanoparticles in powder form was performed during this study.

3.13.1 Characterization of AL NPs in Solution

Dynamic light scattering (DLS) and laser Doppler velocimetry (LDV) techniques were used to characterize AL NPs in solution. The Zetasizer® Nano ZS™ (Malvern® Instruments Inc., Westborough, MA) instrument used a 4 mW He-Ne 633 nm laser and an electric field generator to analyze samples of AL NPs suspended in exposure media. AL NPs at a concentration of 25 μg/mL were suspended, for 24 hours, in deionized water and exposure media. Samples were transferred to a square cuvette for DLS and a Malvern® Clear Zeta Potential cell for LDV. The instrument software used the intensity, volume, and density measurements to calculate the average nanoparticle size. PDI (polydispersity index) is a measure from 0 to 1 of the range of sizes present in the nanoparticle suspension, with 0 meaning monodisperse and 1 meaning polydisperse. Characterization of AL NPs in solution included size, dispersion, zeta potential, and electrophoretic mobility.

3.13.2 Characterization of AL NP Powder

The size and shape of the AL NPs in dry powder form was not performed during this study as it had been characterized during a previous research project. Data on surface area and surface chemistry of AL NPs were obtained from the manufacturer, NovaCentrix™ Inc., Austin, TX.

Surface chemistry characterization was performed to determine if the particles had oxidized since the 2005 purchase. X-ray powder diffraction (XRD) was conducted using a Philips PW1270 Diffractometer (PANalytical Inc., Westborough, MA) to identify layers in the AL NP by measuring the d-spacing, perpendicular space between two planes, and the relative intensity, intensity of the scattered angle. An x-ray beam was aimed at the AL NP, the relative intensity and angle of the scattered rays was measured, and the data was used to calculate the d-spacing. The diffraction data was compared against a database maintained by the International Centre for Diffraction Data. To determine if a carbon coating was present on the AL NPs, the amount, in percent weight, of carbon, hydrogen, and nitrogen was measured using a Leco CHNS 932 elemental analyzer (Leco® Corp., St. Joseph, MI). A sample of AL 50 was placed in a capsule, dropped into the Leco furnace, and heated to 1000°C until the sample was combusted. An infrared detector was used to quantify the amount of carbon, hydrogen, and nitrogen.

3.14 Statistical Analysis

At a minimum, all LDH, MTS, and ROS experiments were performed in triplicate, and the results were presented as mean ± standard deviation. Concentrations were calculated for the LDH, MTS, and ROS data using Microsoft® Excel® (Microsoft® Corp., Seattle, WA). The LDH, MTS, and ROS experimental data were analyzed by ANOVA using Excel®. Statistical significance was accepted at a level of p value ≤ 0.05.

Interleukin-1α and -8 concentration response curves were constructed using four-parameter logistic (4-PL) curve-fit by SigmaPlot® (SYSTAT® Software Inc., San Jose, CA). The interleukin experimental data were analyzed by ANOVA using SigmaPlot® and statistical significance was accepted at a level of p value ≤ 0.05.

The F-test was used to determine if there was a significant difference in the quantities of interleukins expressed by keratinocytes in the presence vs. absence of LPS. The F-test for the interleukin experimental data was performed by ANOVA (single factor) using Excel® and at a 95 percent confidence limit. Table 1 summarizes the experimental hypotheses and the statistical analyses used to test the hypotheses.

Table 1: Hypotheses and Statistical Tests

Assay Experiments Performed	Statistical Analysis Performed
LDH: Necrosis	Student's t-test: Statistical significance, p value ≤ 0.05 H_o: $\mu = 100\%$ (zero control) H_1: $\mu \neq 100\%$
MTS: Cell proliferation	Student's t-test: Statistical significance, p value ≤ 0.05 H_o: $\mu = 100\%$ (zero control) H_1: $\mu \neq 100\%$
ROS: Oxidative stress	Student's t-test: Statistical significance, p value ≤ 0.05 H_o: $\mu = 1$ (zero control) H_1: $\mu \neq 1$
IL-1α: Proinflammatory cytokine and IL-8: Neutrophil and T-lymphocyte attractant	IL-1α Student's t-test: Statistical significance, p value ≤ 0.05 H_o: $\mu = 6.24$ pg/mL (zero control) H_1: $\mu \neq 6.24$ pg/mL Il-8 Student's t-test: Statistical significance, p value ≤ 0.05 H_o: $\mu = 192$ pg/mL (zero control) H_1: $\mu \neq 192$ pg/mL The following were performed on the IL-1α and IL-8 sample data: Zero Control F-test: 95% confidence limit H_o: $s_1^2 = s_2^2$; s_1^2 = zero control w/ LPS; s_2^2 = zero control w/o LPS H_1: $s_1^2 \neq s_2^2$. AL NP Size (nm) F-test: 95% confidence limit H_o: $s_1^2 = s_2^2 = s_3^2$; s_1^2 = AL 50, s_2^2 = AL 80, and s_3^2 = AL 120 H_1: $s_1^2 \neq s_2^2 \neq s_3^2$ Dosing Stock Conc. (µg/ml) F-test: 95% confidence limit H_o: $s_1^2 = s_2^2 = s_3^2 = s_4^2$; $s_1^2 = 10$, $s_2^2 = 100$, $s_3^2 = 1000$, and $s_4^2 = 2000$ H_1: $s_1^2 \neq s_2^2 \neq s_3^2 \neq s_4^2$
Ratio IL-8 to IL-1α	AL NP Size (nm) F-test: 95% confidence limit H_o: $s_1^2 = s_2^2 = s_3^2$; s_1^2 = AL 50, s_2^2 = AL 80, and s_3^2 = AL 120 H_1: $s_1^2 \neq s_2^2 \neq s_3^2$ Dosing Stock Conc. (µg/ml) F-test: 95% confidence limit H_o: $s_1^2 = s_2^2 = s_3^2 = s_4^2$; $s_1^2 = 10$, $s_2^2 = 100$, $s_3^2 = 1000$, and $s_4^2 = 2000$ H_1: $s_1^2 \neq s_2^2 \neq s_3^2 \neq s_4^2$

Note: Student's t-test, two-tailed performed. Statistically significant results were further evaluated to ensure validity.

IV. Data Description and Analysis

4.1 Introduction

The data collected from the research methods described in chapter III is presented in this chapter. Table 2 summarizes the experiments conducted to address the research objectives presented in chapter I.

Table 2. Research Questions and Experiments Performed

Research Objectives	Experiments Performed*
Are AL NPs (50, 80, and 120 nm) toxic to human keratinocytes?	LDH: Necrosis MTS: Cell proliferation
Do AL NPs induce reactive oxygen species?	ROS: Oxidative stress
Do AL NPs induce an inflammatory response in keratinocytes?	LDH: Necrosis ROS: Oxidative stress IL-1α: Proinflammatory cytokine
Can AL NPs be classified as a skin irritant or sensitizer?	IL-8: Neutrophil and T-lymphocyte attractant Ratio of IL-8 to IL-1α

*Cell morphology experiments were performed to determine if cell death was caused by AL NPs or turbidity of dosing stock. Characterization of AL NPs in dosing stock and dry powder form was conducted.

4.2 Keratinocyte Viability Data

The results of the cell viability experiments using LDH, MTS, and ROS assays showed that AL NPs did not induce cell death in human keratinocytes.

4.2.1 LDH Assay Results

Cell membrane leakage of human keratinocytes dosed with AL NPs at concentrations ranging from 10 to 10,000 μg/mL and exposed for 24 hours did not occur (see Figures 4 and 5). The concentration of LDH leaked by keratinocytes dosed with AL NPs did not exceed the concentration of LDH leaked by keratinocytes exposed to 0 μg/mL AL NPs (zero control). The statistically significant (using Student's t-test) data were not likely the result of AL NP exposure because the difference between the mean

LDH result for the zero control and the experimental data was not large, the sample data set was too small to prove that it contained outliers, and the variability within the sample sets was small (Patten, 2005:119). Further evidence of this was demonstrated by the fact that cell membrane leakage was not seen in keratinocytes dosed with concentrations greater than the statistically significant concentration.

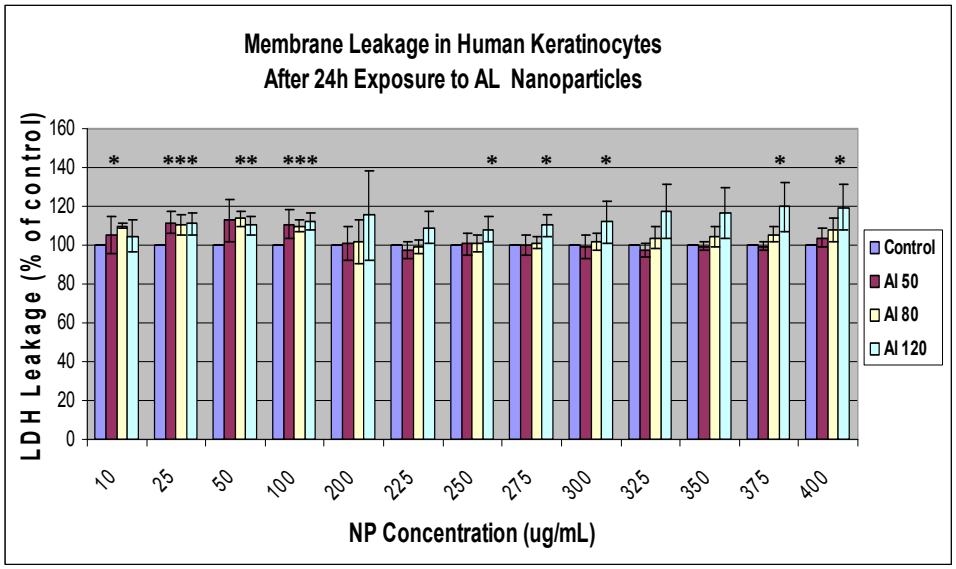

Figure 4. Membrane Leakage in Keratinocytes, AL NP Concentration 10 – 400 µg/mL. Percent LDH increase after 24-hour exposure to AL NPs. * indicates doses that produced LDH results that are significantly different from the zero control, p value ≤ 0.05

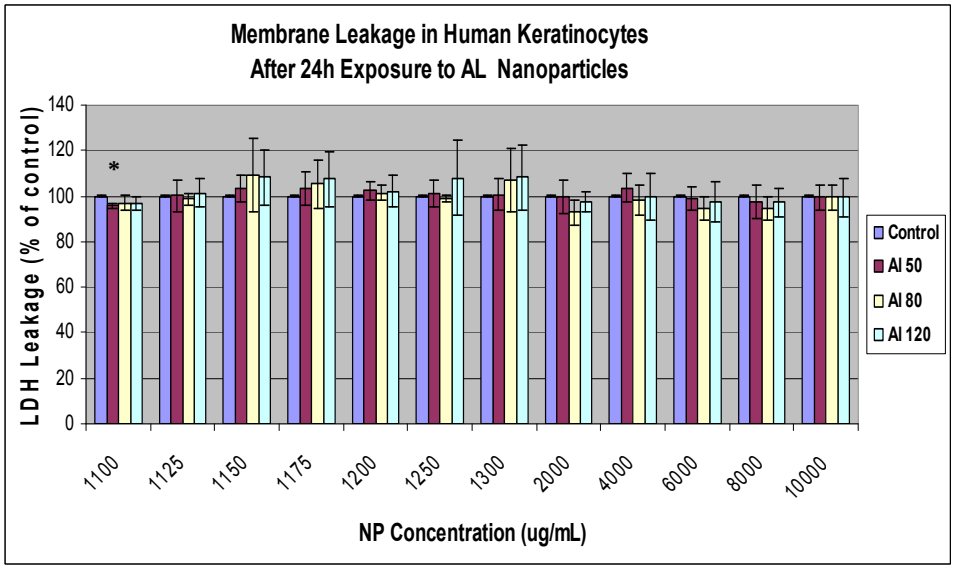

Figure 5. Membrane Leakage in Keratinocytes, AL NP Concentration 1100–10,000 µg/mL. Percent LDH increase after 24-hour exposure to AL NPs. * indicates doses that produced LDH results that are significantly different from the zero control, p value ≤ 0.05

4.2.2 MTS Assay Results

Suppression of mitochondrial function in human keratinocytes, due to 24-hour exposure to AL NPs at concentrations of 10 to 10,000 μg/mL, did not occur (see Figures 6 and 7). The quantity of MTS transformed to formazin by keratinocytes dosed with AL NPs was not significantly lower than MTS transformed to formazin by the zero control keratinocytes. At very high concentrations (> 2000 μg/mL), the MTS results were significantly greater than the zero control results. An experiment was performed to determine if the rise in MTS results were caused by artifact AL NPs. The results showed that there was a statistically significant (p value ≤ 0.05) difference between the two scenarios: rinse, no centrifuge, aliquot, and rinse, centrifuge, aliquot. After the MTS results for keratinocytes dosed with AL NP concentrations > 2000 μg/mL were corrected for nanoparticle fluorescence, the MTS results indicated that high concentrations of AL NPs decreased keratinocyte proliferation. Correcting the MTS results for fluorescence removed any random bias that may have resulted from the inconsistent use of the centrifuge. However, the results of cell morphology experiments (see paragraph 4.3) indicate that decreased cell proliferation was not caused by the nanoparticles, but by the turbidity of the dosing stock. The statistically significant (using Student's t-test) data were not likely the result of AL NP exposure because the difference between the mean MTS result for the zero control and the experimental data was not large, the sample data set was too small to prove that it contained outliers, and the variability within the sample data sets was small (Patten, 2005:119). Further evidence that AL NPs did not reduce cell proliferation was demonstrated by the fact that a decrease in mitochondrial function was

not seen in keratinocytes dosed with concentrations greater than the statistically significant concentration.

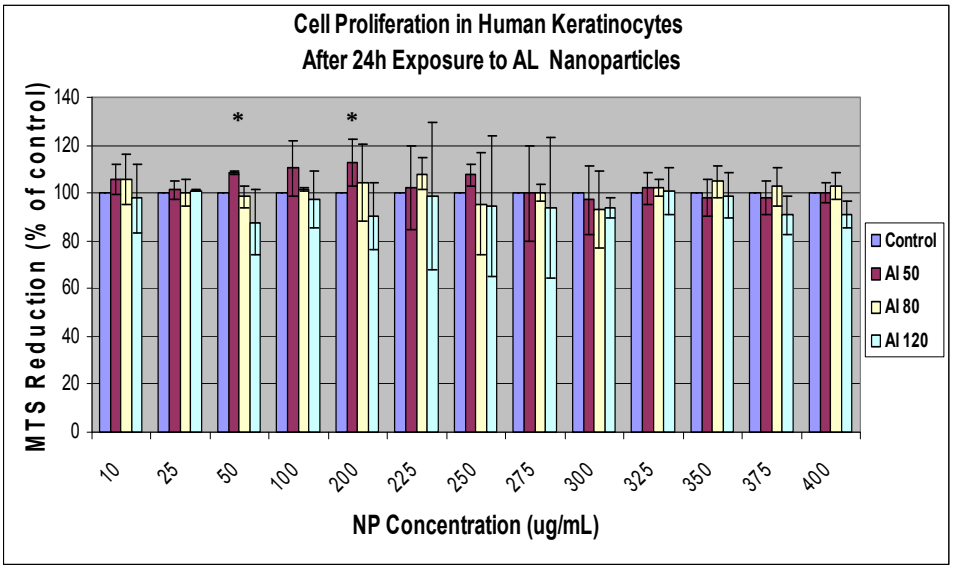

Figure 6. Cell Proliferation in Keratinocytes, AL NP Concentration 10 – 400 µg/mL. Percent MTS decrease after 24-hour exposure to AL NPs. * indicates doses that produced MTS results that are significantly different from the zero control, p value ≤ 0.05

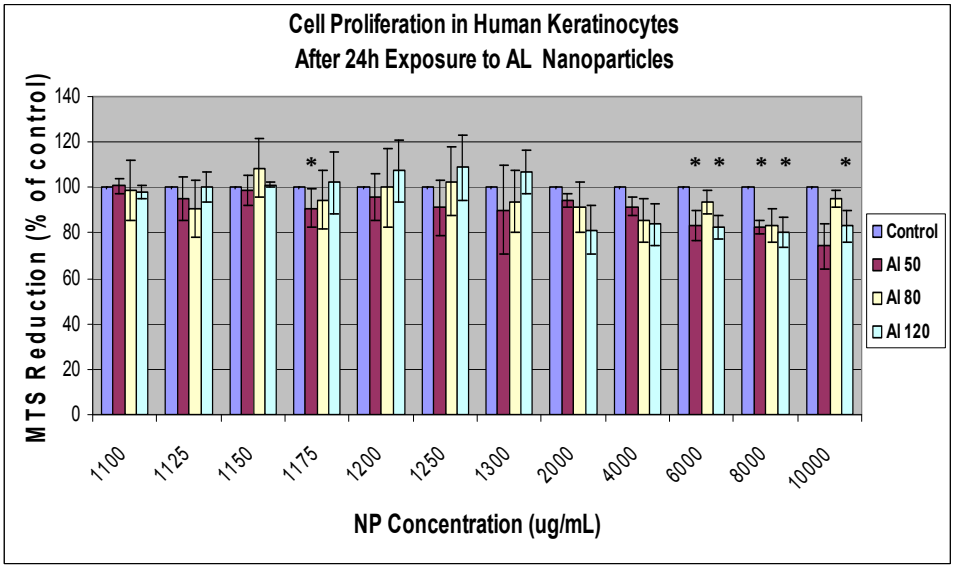

Figure 7. Cell Proliferation in Keratinocytes, AL NP Concentration 1100 – 10,000 µg/mL. Percent MTS decrease after 24-hour exposure to AL NPs. * indicates doses that produced MTS results that are significantly different from the zero control, p value ≤ 0.05

4.2.3 ROS Assay Results

The keratinocyte generation of the ROS during a 24-hour exposure to AL NPs at concentrations 10, 100, 500, 1000, and 2000 µg/mL was not significant (see Figure 8). Although cell death occurred at concentrations > 2000 µg/mL, ROS experiments were not performed for those concentrations because the turbidity of the dosing stock vs. the AL NPs was the cause of the decrease in cell proliferation. The concentrations of ROS generated by keratinocytes exposed AL NPs were not statistically significant (p value > 0.05) when compared to the ROS concentration generated by keratinocytes exposed to 0 µg/mL AL NPs (zero control). Student's t-test was performed to compare the ROS data generated by AL NP size, by exposure time, and by concentration of dosing stock against the zero control, the results of all were not statistically significant (p value > 0.05).

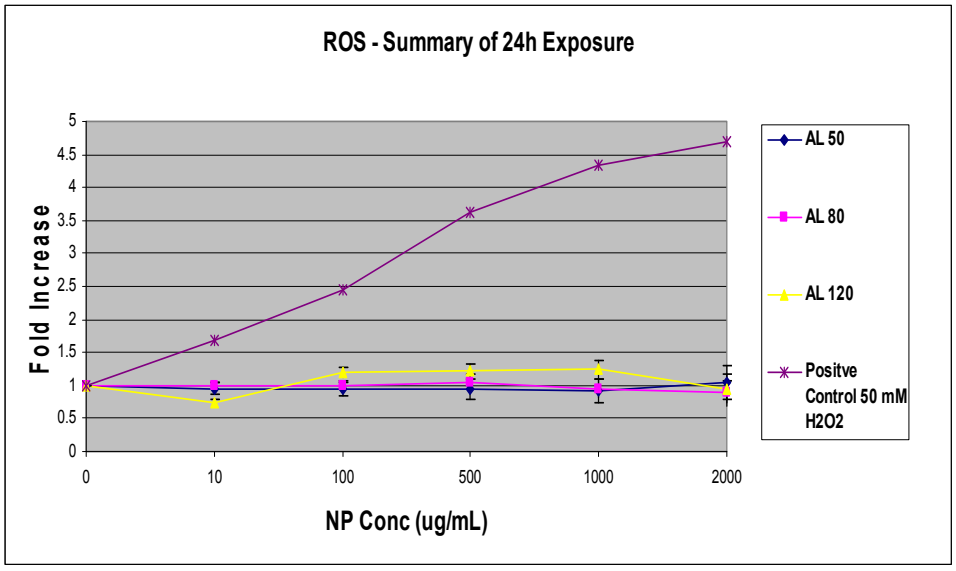

Figure 8. Summary of Reactive Oxygen Species. Generation of ROS from keratinocytes after 24-hour exposure to AL NPs. H_2O_2 used as positive control.

4.3 Keratinocyte Morphology Results

Pictures were taken of keratinocytes after 24-hour exposure to AL NPs or talc using an Olympus1x71 inverted microscope at 10x1.6 magnification (see Figures 9 and 10).

The blank spaces in the cell morphology pictures, in comparison to the 100 percent confluent cells in the zero controls (A), represent cell death that occurred when keratinocytes were dosed with AL NPs or talc at concentrations 2000, 4000, 6000, 8000, and 10,000 µg/mL.

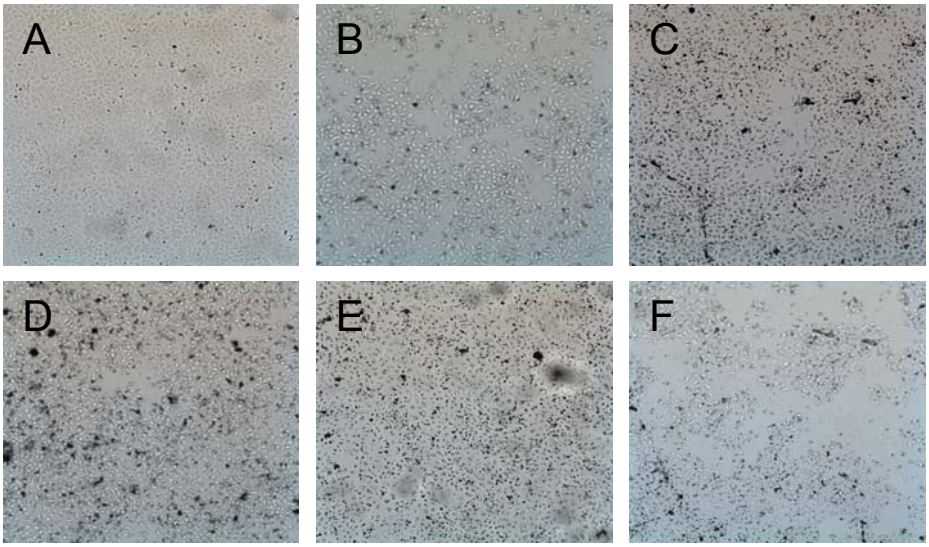

Figure 9. Keratinocyte Morphology, AL NP Concentration. A) zero control, 0 µg/mL, B) 80 nm at 2000 µg/mL, C) 120 nm at 4000 µg/mL, D) 50 nm at 6000 µg/mL, E) 80 nm at 8000 µg/mL, and F) 120 nm at 10,000 µg/mL, Olympus1x71 inverted microscope, 10x1.6 magnification

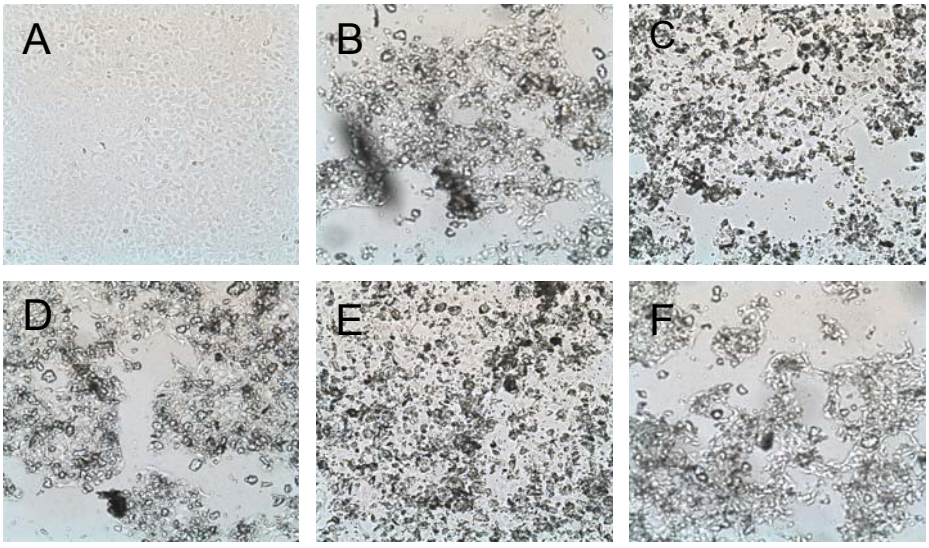

Figure 10. Keratinocyte Morphology, Talc Concentration. A) zero control, 0 µg/mL, B) 2000 µg/mL, C) 4000 µg/mL, D) 6000 µg/mL, E) 8000 µg/mL, and F) 10,000 µg/mL. Olympus 1x71 inverted microscope, 10x1.6 magnification

MTS was performed to verify if the blank spaces represented dead cells. The MTS results for keratinocytes dosed with talc showed that there was a significant drop in cell proliferation (see Figure 11). The pH measurements for the AL NP and talc dosing stocks, the exposure media, unexposed cells in exposure media, and cells supernate with nanoparticles (after 24-hour exposure) were 8. Since there was no change, pH did not contribute to cell death.

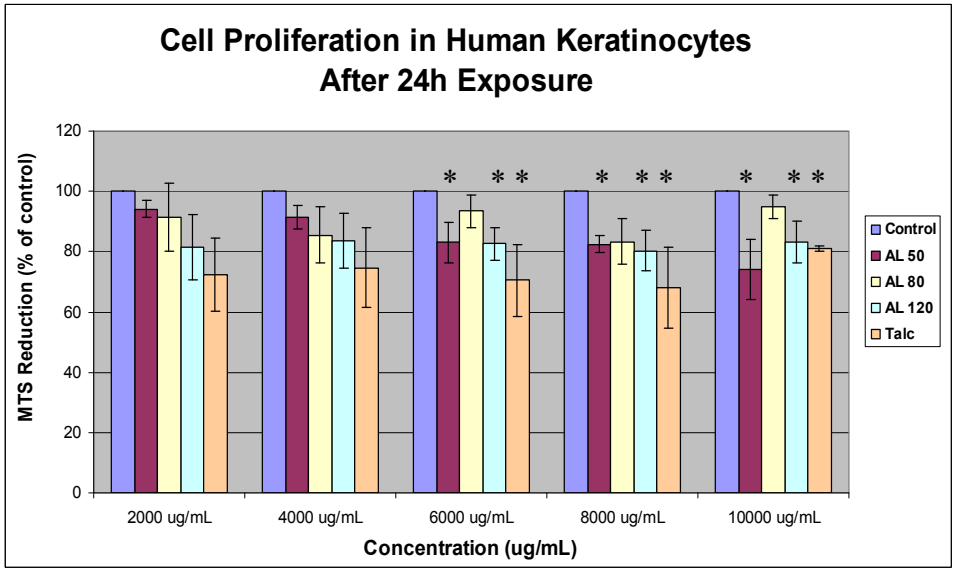

Figure 11. Cell Proliferation in Keratinocytes, AL NP and Talc Concentration 2000 – 10,000 μg/mL. Percent MTS decrease after 24-hour exposure to AL NPs. * indicates doses that produced MTS results that are significantly different than the zero control, p value ≤ 0.05

Characterization of talc particle size, its zeta potential, and its electrophoretic mobility in solution was performed using DLS and LDV (see Table 3 for results). The mean particle size of the talc suspended in exposure media (after 24 hours) was 2600 nm, greater than 100 nm, and was not a nanosized material. Talc suspended in exposure media agglomerated to an average size that was 15 percent larger than talc particles suspended in distilled water. The polydispersity index (PDI) for the talc suspended in

distilled water and exposure media was 1, indicating that the size of the particles dispersed in these solutions were very diverse.

Zeta potential and electrophoretic mobility are a measure of the stability of the particle in suspension (see paragraph 4.5.1 for more details). The talc particles suspended in distilled water (for 24 hours) were unstable and likely to agglomerate because the zeta potential was less than ± 30 mV (Wagner and others, 2007:7357). The zeta potential and electrophoretic mobility of talc suspended in exposure media could not be measured because the high salt concentrations of the RPMI cause corrosion of the sample chamber electrodes.

Table 3. Characterization of Talc in Solution

Particle	DLS		LDV		pH
	mean diameter (nm)	PDI	zeta potential ζ (mV)	electrophoretic mobility μ ($\mu m \cdot cm \cdot V^{-1} \cdot s^{-1}$)	
*Talc (in solution for 24 hours)					
DI H_2O	2220	1	-23.1	-1.81	
RPMI w/ 1% pen/strep	2600	1			8

Measured at concentration 25 μg/mL, maximum concentration allowed for method. *Solution at 25 °C.

4.4 Keratinocyte Interleukin Expression Data

Interleukin-1α and -8 extracellular expressions by keratinocytes were quantified using R & D Systems®, Inc., ELISA immunoassay kits.

4.4.1 IL-1α Extracellular Expression

The F-test ($F_{Calc} < F_{Critical}$) proved, with a 95 percent confidence, that there was no statistical difference in the concentration results of the two IL-1α zero controls (with and without LPS). Because the data from the two zero controls is virtually the same, it is not

likely that the LPS induced the extracellular expression of IL-1α in the controls Using Student's t-test, all IL-1α results proved statistically significant (p value ≤ 0.05) when compared with the IL-1α zero control (see Figure 12).

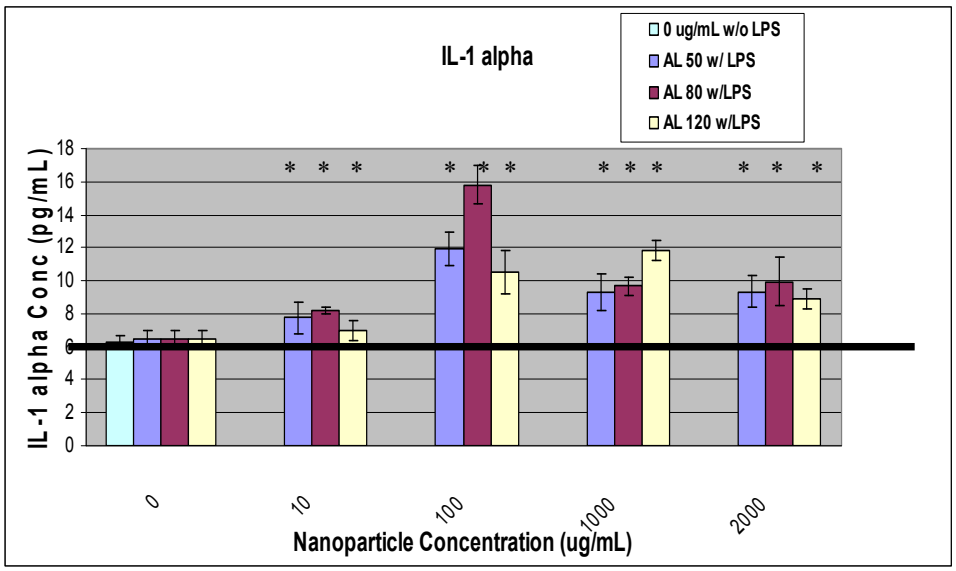

Figure 12. Results of Extracellular IL-1α Expression. IL-1α expressed after 24-hour exposure to AL NPs. * indicates IL-1α results that are significantly different than the IL-1α results produced by zero control, p value ≤ 0.05 (data used in developing graph not corrected for zero control)

4.4.2 IL-8 Extracellular Expression

The F-test ($F_{Calc} > F_{Critical}$) proved, with a 95 percent confidence, that there was statistical difference in the results of the two IL-8 zero controls (with and without LPS). Because the concentration of IL-8 is dramatically higher in the LPS zero control it is likely that the LPS aided the IL-1α in the extracellular expression of IL-8. Using Student's t-test, all IL-8 results, except AL 50 at 10 µg/mL, proved to be statistically significant (p value ≤ 0.05) when compared with the LPS zero control (see Figure 13). The calculated p value for the AL 50 at 10 µg/mL data set was 0.179. The data set for

AL 50 at 10 µg/mL was too small to prove that it contained outliers and may have been the reason that the IL-8 results were not statistically significant (*p* value > 0.05).

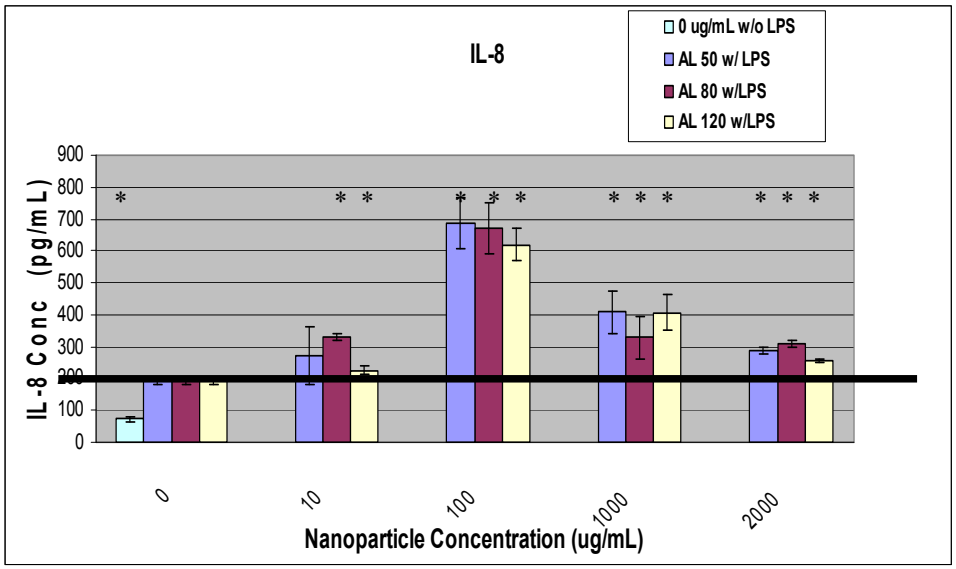

Figure 13. Results of Extracellular IL-8 Expression. IL-8 expressed after 24-hour exposure to AL NPs. * indicates IL-8 results that are significantly different than the IL-8 results produced by zero control, *p* value ≤ 0.05 (data used in developing graph not corrected for zero control)

4.4.3 Comparison of IL-1α and IL-8 Results

Table 4 is a summary of the MTS percent reduction, IL-1α and IL- 8 results, and the ratio of IL-8 to IL-1α. Statistical analysis (ANOVA, Single Factor) of the IL-1α and IL-8 concentrations expressed by each AL NP size indicated that the data, with 95 percent confidence, is statistically equal ($F_{Calc} < F_{Critical}$). However, statistical analysis (ANOVA, Single Factor) of the IL-1α and IL-8 concentrations associated with each dosing concentration indicates that the data, with 95 percent confidence, is statistically different ($F_{Calc} > F_{Critical}$).

Table 4. MTS Percent Reduction and Extracellular Interleukin Concentration

Particle, Concentration (μg/mL)	MTS % Reduction ± Std Dev	Mean IL-1α (pg/mL	Corrected[a] Mean IL-1α (pg/mL)	Mean IL-8 (pg/mL) w/LPS	Corrected[b] Mean IL-8 (pg/mL)	Ratio[c] IL-8 / IL-1α
AL 50, 10	105.93 ± 6.34	7.76 ± 0.59	1.52	272 ± 91	80	52.3
AL 50, 100	110.53 ± 11.55	11.95 ± 0.64	5.70	687 ± 78	495	86.8
AL 50, 1000*	100.86 ± 3.11	9.34 ± 0.74	3.09	408 ± 70	216	69.9
AL 50, 2000	94.21 ± 2.73	9.33 ± 0.59	3.09	286 ± 13	94	30.3
AL 80, 10	105.89 ± 10.55	8.20 ± 0.18	1.95	330 ± 8	138	70.8
AL 80, 100	101.60 ± 0.79	15.82 ± 0.78	9.58	670 ± 81	478	49.9
AL 80, 1000*	98.65 ± 13.19	9.67 ± 0.21	3.42	329 ± 67	137	40.0
AL 80, 2000	91.35 ± 11.32	9.94 ± 1.06	3.70	311 ± 10	119	32.1
AL 120, 10	97.69 ± 14.08	6.97 ± 0.22	0.73	225 ± 13	33	44.6
AL 120, 100	97.08 ± 11.97	10.51 ± 0.91	4.27	620 ± 51	427	100.2
AL 120, 1000*	97.82 ± 2.85	11.82 ± 0.19	5.57	407 ± 56	215	38.5
AL 120, 2000	81.35 ± 10.79	8.87 ± 0.23	2.62	256 ± 6	64	24.5

*MTS results for AL NP concentration of 1100 μg/mL
[a]Corrected mean IL-1α results = IL-1α results minus 6.24 (zero control)
[b]Corected mean IL-8 results = IL-8 (w/LPS) minus 192 pg/mL (zero control w/ LPS)
[c]Ratio of corrected means

Figure 14 contains two graphs plotting the ratio of IL-8 to IL-1α against AL NP size, and the ratio against AL NP concentration. Statistical analysis (ANOVA, Single Factor) of the ratio of IL-8 to IL-1α by each AL NP size indicated that the data, with 95 percent confidence, is statistically equal ($F_{Calc} < F_{Critical}$). However, statistical analysis (ANOVA, Single Factor) of the ratio of IL-8 to IL-1α by each dosing concentration indicates that the data, with 95 percent confidence, is statistically different ($F_{Calc} > F_{Critical}$).

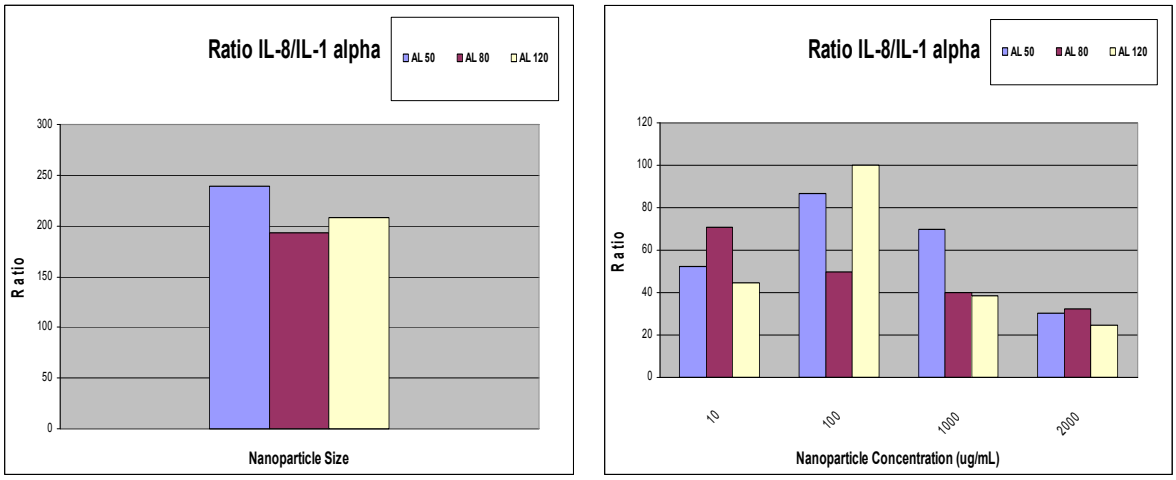

Figure 14. Ratio of IL-8 to IL-1α. By AL NP size (left). By AL NP dosing stock concentration (right).

4.5 Aluminum Nanoparticle Characterization Results

Characterization of size, dispersion, and chemical and physical properties was conducted for particles suspended in exposure media. The surface chemistry of particles in dry powder form was also performed.

4.5.1 Characterization of AL NPs in Solution

Characterization of nanoparticle size, its zeta potential, and its electrophoretic mobility in solution was performed using DLS and LDV (see Table 5 for results). AL NPs suspended for 24 hours in exposure media and in distilled water agglomerated, and formed particles that were greater than 100 nm. The mean agglomerated particle size of the AL NPs suspended in exposure media ranged from 755 – 959 nm. AL NPs suspended in exposure media agglomerated to sizes 53 (AL 120) – 67 (AL 50) percent larger than the sizes of the agglomerated particles in the distilled water. The PDI for all three nanoparticles indicated that there was not a variety of size ranges present in the distilled water and exposure media suspensions.

Table 5. Characterization of AL NPs in Solution

Particle	DLS		LDV		pH
	mean diameter (nm)	PDI	zeta potential ζ (mV)	electrophoretic mobility μ ($\mu m \cdot cm \cdot V^{-1} \cdot s^{-1}$)	
*AL 50 nm (in solution for 24 hours)					
DI H_2O	316	0.241	-18.2	-1.42	
RPMI w/ 1% pen/strep	959	0.339			8
*AL 80 (in solution for 24 hours)					
DI H_2O	291	0.223	-21.7	-1.7	
RPMI w/ 1% pen/strep	755	0.309			8
*AL 120 (in solution for 24 hours)					
DI H_2O	378	0.322	-26.2	-2.05	
RPMI w/ 1% pen/strep	806	0.342			8

Measured at concentration 25 μg/mL, maximum concentration allowed for method. *Solution at 25 °C.

Zeta potential (surface charge) was calculated from the measured electrophoretic mobility of the particle. Electrophoretic mobility was the surface electrical charge of the particle in relation to its movement within fluid in which it was suspended (Zeta Potential, 2008:3). The zeta potential is used to categorize the stability of a particle based on its ability to remain in solution. AL NPs suspended in the distilled water were unstable and likely to agglomerate because the zeta potential for all three sizes was less than ± 30 mV with AL 50 (-18 mV) being less stable than AL 120 (-26 mV). The concentration of the particles in solution may have contributed to the instability of the particles because as the solution becomes more turbid, the zeta potential decreases (Zeta Potential, 2008:8). Table 6 outlines the range of zeta potentials and the corresponding colloid stability. The zeta potential and electrophoretic mobility of particles suspended in exposure media could not be measured because the high salt concentrations of the RPMI cause corrosion of the sample chamber electrodes.

Table 6. Zeta Potential and Colloid Behavior (Adapted from ASTM Std D4187-82)

Zeta Potential (mV)	Stability Behavior of the Colloid
from 0 to ±5	Rapid coagulation or flocculation
from ±10 to ±30	Incipient instability
from ±30 to ±40	Moderate stability
from ±40 to ±60	Good stability
more than ±61	Excellent stability

4.5.2 Characterization of AL NPs in Powder

Data on the size of the AL NPs in dry powder form was adopted from Wagner's article "Cellular Interaction of Different Forms of Aluminum Nanoparticles in Rat Alveolar Macrophages" because the particles used in this study came from the same jars used in his research (see Table 7).

Table 7. Characterization of AL NP Powder (adapted from Wagner, 2007:7354)

Particle and Size Provided by Manufacturer (nm)	Mean Diameter (nm)	Standard Deviation (nm)
AL 50 nm	40.2	± 17.3
AL 80 nm	67.2	± 26.3
AL 120 nm	110	± 34.1

Mean diameter and standard deviation determined by measuring 100 particles using TEM.

The mean particle diameter was 8 – 20 percent smaller than the size claimed by the manufacturer, NovaCentrix™. However, the manufacturer's size fell within the standard deviation determined by Wagner's research. NovaCentrix™ classifies these particles as spherical and crystalline (see Figure 15).

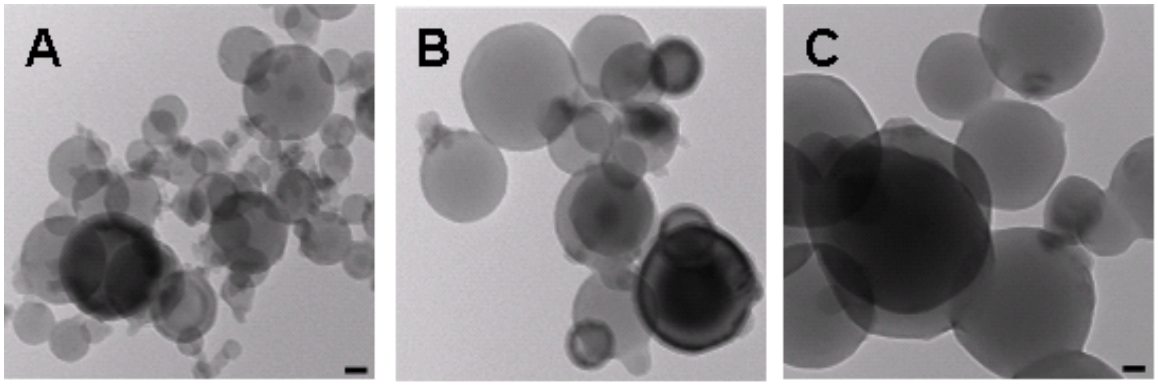

Figure 15: Transmission Electron Microscopy of Aluminum Nanoparticles. Nanoparticles were suspended in distilled water and deposited onto formvar/carbon-coated TEM grids. A) AL 50 nm, B) AL 80 nm, C) AL 120 nm. Photo courtesy of AFRL/RHPB

Data on particle surface area and surface chemistry were obtained from the manufacturer, NovaCentrix™. The data from NovaCentrix™ was validated by surface chemistry analysis performed using XRD and combustion in an elemental furnace. Surface chemistry analysis was performed to determine if the nanoparticles had oxidized since the 2005 purchase. Per Dr. Schrand, the oxide coating created by the manufacturer had not increased (personal communication, 30 November 2007). See Table 8 for surface area and oxide coating information.

Table 8. Surface Area and Oxide Coating (adapted from NovaCentrix™, 2007)

Particle and Size Provided by Manufacturer (nm)	Mean Surface Area Provided by Manufacturer (m^2/g)	Thickness of Oxide Coating (nm)*
AL 50 nm	44	1 – 2
AL 80 nm	28	1.5 – 2.5
AL 120 nm	18	1.5 – 2.5

Mean diameter, surface area, and oxide coating characterized by NovaCentrix™ Inc. using XRD, TEM, and BET. AL NPs manufactured with oxide coating to minimize spontaneous combustion. NovaCentrix™ characterized the nanoparticles as spherical and crystalline. This was confirmed by Wagner, 2007:7354 using TEM. *Results from University of Dayton show no additional oxidation.

V. Conclusions and Future Research Considerations

5.1 Overview

This chapter provides a discussion of the results of this study, suggests methodology improvements, recommends additional research on the effects of aluminum nanoparticles on human skin, and discusses future occupational health concerns.

5.2 Discussion

Results of the experiments performed to assess keratinocyte viability and interleukin response are summarized below. The cell morphology experiments and the AL NP characterization are also discussed in this section.

5.2.1 Cell Viability

Table 9 is a summary of the first and second research objectives of this study, the statistical tests used to validate the experimental data, and the results of these tests.

Table 9. Summary of Research Objectives 1 and 2

Research Objective 1 Are AL NPs (50, 80, and 120 nm) toxic to human keratinocytes?	
Student's t-test: Statistical significance, p value ≤ 0.05 H_o: $\mu = 100\%$ (zero control) H_1: $\mu \neq 100\%$	Necrosis - LDH: all results p value > 0.05 Cell Proliferation - MTS: all results p value > 0.05
Research Objective 2 Do AL NPs induce reactive oxygen species?	
Student's t-test: Statistical significance, p value ≤ 0.05 H_o: $\mu = 1$ (zero control) H_1: $\mu \neq 1$	Oxidative Stress - ROS: all results p value > 0.05

Cell membrane integrity was evaluated by quantifying a colorimetric reaction to measure the concentration of LDH, a component of the cytoplasm of eukaryotic cells, to determine if the cell membrane had been compromised. The colorimetric reaction occurs

when LDH reacts with an assay enzyme that converts a dye, resazurin, to resorufin (TB306, 2007:2). All experimental results were compared to the results of a zero control. The comparison of the experimental data to the zero control data proved that the data was not statistically significant; therefore, AL NPs did not compromise the cell membranes of the keratinocytes.

Cell metabolic activity was evaluated by quantifying a colorimetric reaction to measure the conversion of MTS to formazan, which is a result of mitochondrial function. Reduced mitochondrial function indicates that the cells were not proliferating as the mitochondria in healthy, living cells convert MTS to formazan (TB169, 2005:1). All experimental results were compared to the results of a zero control. The comparison of the experimental data to the zero control data proved that the data was not statistically significant, therefore, AL NPs did not reduce cell proliferation.

The answer to research objective 1 is no. Cell membrane integrity and metabolic activity were the parameters used to assess keratinocyte viability after exposure to AL NPs (50, 80, and 120 nm) at concentrations ranging from 10 to 10,000 μg/mL for 24 hours. The comparison of the LDH and MTS experimental data to the zero control proved that the experimental data was not statistically significant; therefore, AL NPs, with the charge and surface chemistry of the particles used in this study, did not cause cell necrosis nor reduce cell proliferation.

Oxidative stress occurs when the concentration of the ROS generated by the cell, exceeds the cell's antioxidant defenses (Xia and others, 2006:1795). Cell damage occurs when ROS are converted to hydroxyl radicals, which can cause cell necrosis or induce

apoptosis by damaging cell DNA, cell organelles, and cell membranes. The cell damage caused by the ROS may induce inflammation in surrounding tissue.

The answer for research objective 2 is no. Keratinocyte generation of the ROS during a 24-hour exposure to AL NPs (50, 80, and 120 nm) at concentrations 10, 100, 500, 1000, and 2000 μg/mL was not statistically significant. The statistical analysis of the data by AL NP size, by exposure time, and by concentration of the dosing stock showed that these were not factors in ROS generation. AL NPs, with the charge and surface chemistry of the particles used in this study, did not induce ROS generation.

5.2.2 Cell Morphology

Changes to keratinocyte morphology were assessed to determine if AL NPs at concentrations > 2000 μg/mL were the cause of reduced cell proliferation. Keratinocytes were dosed with like concentrations of talc and changes in cell growth were compared with a zero control. An MTS experiment was performed to confirm reduced cell proliferation. The results of this experiment show that the reduction in cell proliferation was not caused by the AL NPs, but by the turbidity of the dosing stock.

5.2.3 Interleukin Response

Concentrations of IL-1α and -8, expressed after 24-hour exposure to AL NPs (50, 80, and 120 nm) at concentrations 10, 100, 500, 1000, and 2000 μg/mL and LPS, was quantified using colorimetric ELISA immunoassays. Table 10 is a summary of the third and fourth research objectives of this study, the statistical tests used to validate the experimental data, and the results of these tests.

Table 10. Summary of Research Objectives 3 and 4

Research Objective 3 Do AL NPs induce an inflammatory response in keratinocytes?	
	Necrosis - LDH: all results p value > 0.05 Oxidative Stress - ROS: AL 120 p value ≤ 0.05, oxidative stress occurred AL 50 and AL 80 p value > 0.05
	Proinflammatory Cytokine IL-1α:
Zero Control F-test: 95% confidence limit H_o: $s_1^2 = s_2^2$; s_1^2 = zero control w/ LPS; s_2^2 = zero control w/o LPS H_1: $s_1^2 \neq s_2^2$	Zero Control F-test: $F_{Calc} < F_{Critical}$, No statistical difference
Student's t-test: Statistical significance, p value ≤ 0.05 H_o: μ = 6.24 pg/mL (zero control) H_1: μ ≠ 6.24 pg/mL	Student's t-test: p value ≤ 0.05, sample data statistically different from zero control
AL NP Size (um) F-test: 95% confidence limit H_o: $s_1^2 = s_2^2 = s_3^2$; s_1^2 = AL 50, s_2^2 = AL 80, and s_3^2 = AL 120 H_1: $s_1^2 \neq s_2^2 \neq s_3^2$	AL NP Size F-test: $F_{Calc} < F_{Critical}$, No statistical difference
Dosing Stock Conc. (μg/ml) F-test: 95% confidence limit H_o: $s_1^2 = s_2^2 = s_3^2 = s_4^2$; s_1^2 = 10, s_2^2 = 100, s_3^2 = 1000, and s_4^2 = 2000 H_1: $s_1^2 \neq s_2^2 \neq s_3^2 \neq s_4^2$;	Dosing Stock F-test: $F_{Calc} > F_{Critical}$, Statistically different
Research Objective 4 Can AL NPs be classified as a skin irritant or sensitizer?	
	Neutrophil and T-lymphocyte attractant IL-8:
Zero Control F-test: 95% confidence limit H_o: $s_1^2 = s_2^2$; s_1^2 = zero control w/ LPS and s_2^2 = zero control w/o LPS H_1: $s_1^2 \neq s_2^2$	Zero Control F-test: $F_{Calc} > F_{Critical}$, Statistically different
Student's t-test: Statistical significance, p value ≤ 0.05 H_o: μ = 192 pg/mL (zero control) H_1: μ ≠ 192 pg/mL	Student's t-test: p value ≤ 0.05, sample data statistically different from zero control
AL NP Size (nm) F-test: 95% confidence limit H_o: $s_1^2 = s_2^2 = s_3^2$; s_1^2 = AL 50, s_2^2 = AL 80, and s_3^2 = AL 120 H_1: $s_1^2 \neq s_2^2 \neq s_3^2$	AL NP Size F-test: $F_{Calc} < F_{Critical}$, No statistical difference
Dosing Stock Conc. (μg/ml) F-test: 95% confidence limit H_o: $s_1^2 = s_2^2 = s_3^2 = s_4^2$; s_1^2 = 10, s_2^2 = 100, s_3^2 = 1000, and s_4^2 = 2000 H_1: $s_1^2 \neq s_2^2 \neq s_3^2 \neq s_4^2$;	Dosing Stock F-test: $F_{Calc} > F_{Critical}$, Statistically different
	Ratio of IL-8 to IL-1α
	AL NP Size F-test: $F_{Calc} < F_{Critical}$, No statistical difference
	Dosing Stock F-test: $F_{Calc} > F_{Critical}$, Statistically different

IL-1α is synthesized by the mitochondria (Coquette and others, 1999:875) and IL-8 is synthesized when the nuclear factor-kappa beta (NF-Kβ) is activated by protein kinase C (Chabot-Fletcher and others, 1994:509). IL-1α initiates the inflammation process when released from the cells. IL-1α may be released when the cell membrane is compromised or when the cell is stimulated. Since the LDH experiments proved that the AL NPs did not cause cell membrane rupture, the concentrations of IL-1α measured during this experiment were expressed by stimulated keratinocytes. The IL-1α concentrations, expressed by keratinocytes dosed with AL 50 and AL 80 at the concentration of 100 μg/mL, were 5.70 and 9.58 pg/mL, respectively. AL 120 at 1000 μg/mL produced 5.57 pg/mL, which was slightly larger than the 4.27 pg/mL expressed after exposure to AL 120 at 100 μg/mL. There was no significant difference between the IL-1α concentrations expressed by size, however, there was a significant difference between the IL-1α concentrations expressed by concentration of the dosing stock. Therefore, keratinocyte expression of IL-1α was dose dependent vs. nanoparticle size dependent. The lower concentrations of IL-1α expressed by keratinocytes dosed with 2000 μg/mL were likely caused by the turbidity of the dosing stock. The turbidity of the dosing stock may have reduced mitochondrial function, or blocked the LPS from reaching and stimulating the cells. All IL-1α concentrations released in this experiment, except for AL 80 at 100 μg/mL, fall just below the range of IL-1α concentrations measured in the *in vitro* experiments performed by Coquette and others. Per Coquette and others, keratinocytes dosed with sensitizer agents (0.414 – 14.7 mg/mL) expressed IL-1α in the range of 6 to 35 pg/mL, and dosed with irritant agents (1.62 – 36.6 mg/mL) expressed IL-1α in the range of 46.5 to 236 pg/mL (Coquette and others, 2003:314-316).

The answer for research objective 3 is no. Based on the concentrations of LDH, ROS, and IL-1α measured in this research, the keratinocytes did not exhibit an inflammatory response.

In addition to initiating the inflammation process, IL-1α stimulates the release of secondary mediators, including IL-8. IL-8 is a chemotactic that signals neutrophils and T-lymphocytes to the cell to begin phagocytosis. The relatively low concentration of IL-8 measured in the without-LPS zero control indicates that LPS, in combination with IL-1α, stimulated keratinocyte release of IL-8. Keratinocytes exposed to the AL NP dosing stock of 100 μg/mL produced the highest concentration of IL-8. AL 50, AL 80, and AL 120, produced extracellular concentrations at 495, 478, and 427 pg/mL, respectively. There was no significant difference between the IL-8 concentrations expressed by nanoparticle size, however, there was a significant difference between the IL-8 concentrations expressed by concentration of the dosing stock. Therefore, keratinocyte expression of IL-8 was dose dependent vs. nanoparticle size dependent. The low concentration of IL-8 expressed by keratinocytes dosed to 2000 μg/mL was likely due to the decrease in IL-1α concentrations. The IL-8 concentrations released by keratinocytes exposed to AL 50, AL 80, and AL 120 at 100 and 1000 μg/mL fall within the range of IL-8 concentrations measured in the *in vitro* experiments performed by Coquette and others. Per Coquette and others, keratinocytes dosed with sensitizer agents (0.414 – 14.7 mg/mL) expressed IL-8 in the range of 164 to 495 pg/mL, and dosed with irritant agents (1.62 – 36.6 mg/mL) expressed IL-8 in the range of 21 to 168 pg/mL (Coquette and others, 2003:314-316).

The ratio of IL-8 to IL-1α ranged from 24.5 to 100.2. AL NP dosing concentrations of 100 μg/mL produced ratios ranging from 86.8 to 100.2, with AL 120 producing the highest ratio. The ratio for AL 80 at 10 μg/mL was 70.8, larger than the ratio produced at 100μg/mL, and the ratio for AL 50 at 1000 μg/ml was 69.9, larger than the ratio produced by AL 80 at 100 μg/mL. The ratios of IL-8 to IL-1α concentrations reported by Coquette and others ranged from 8.4 to 41.0 for sensitizers and 0.2 to 0.7 for irritants (Coquette and others, 2003:314-316). Despite the higher ratio produced by the AL 50 and AL 80, statistical analysis of the ratios show that the ratios were dose dependent vs. nanoparticle size dependent.

The answer for research objective 4 is yes. Based on the concentrations of IL-1α, IL-8, and the corresponding ratios AL NP can be categorized as a skin sensitizer. This conclusion is also supported by the fact that aluminum is considered a mild, but rare sensitizer that causes SRD in susceptible populations.

5.2.4 Nanoparticle Characterization

Characterization of nanoparticle size, its zeta potential, its electrophoretic mobility in solution, and dry powder surface chemistry was performed using DLS, LDV, and XRD. AL NPs suspended for 24 hours in exposure media and in distilled water, agglomerated and formed particles that were greater than 100 nm. The particle charge and surface chemistry of the AL NPs used in this study did not make the particles toxic to human keratinocytes.

5.3 Suggested Methodology Improvements

There are several suggestions that could improve the methodologies used in this research and lend strength to the results of this study. These suggestions include (1) time

and concentration studies to identify the optimal concentration of LPS to use in the interleukin experiments; (2) time studies to determine if IL-1α and IL-8 expression occurs soon after exposure or increases/decreases over time; (3) keratinocyte uptake of AL NPs; (4) the use of nanosized materials of known sensitizers and irritants as controls to compare against AL NP induced interleukin expression; and (5) the replacement of the HaCaT keratinocyte model with a skin cell model that includes Langerhans cells for HLA-DR imaging.

The concentration of LPS used in this study (25 μg/mL for a 24-hour exposure) was selected based on published studies that used 100 μg/mL for a 6-hour exposure. This rationale may not have ensured the maximum expression of IL-1α and IL-8. Time and concentration studies would have identified the concentration of LPS needed to induce optimal interleukin expression during the 24-hour exposure period.

Performing time studies on keratinocyte extracellular expression of IL-1α and IL-8 may show when, after AL NP exposure, cells may become susceptible to SRD. The experiments performed in this study do not prove when, during the 24-hour exposure, cells may have been more susceptible to an SRD agent. In the time studies performed by Kristensen and others, keratinocyte expression of IL-8 peaked at 4 hours, decreasing to its lowest concentration at 10 hours, and rising again until at 24 hours the concentration is roughly 50 percent of concentration seen at 4 hours.

Keratinocyte uptake of AL NPs was not performed during this study. Transmission electron microscopy imagining of cells after dosing and incubation should be performed to determine if the AL NPs adhere to the outside of the cell membrane or migrate through the membrane to interact with the organelles.

In this study, there were no experiments performed using known ICD or SRD agents. Dosing keratinocytes at concentrations greater than and less than cytotoxic doses, with nanosized materials of known sensitizers (e.g. nickel) and irritants (e.g. copper), and quantifying expressed IL-1α and IL-8 using the R & D Systems®, Inc. assay kits would help validate the results of this research.

The HaCaT cell line used in this study did not contain Langerhans cells, which are dendritic, or immune system cells that reside in the epidermis. HLA-DR is a major histocompatibility complex, MHC class II, cell surface receptor found on immune system cells that aid or suppress recruitment of T-lymphocytes. Confocal and electron microscopy show that Langerhans cells exposed to sensitizer agents internalized HLA-DR molecules in lysosomes near the nucleus. When exposed to an irritant agent, the Langerhans cells internalized the HLA-DR in prelysosomes near the cell membrane (Ale and Maibach, 2004:246). This imaging would validate the interleukin response of the keratinocytes and confirm that AL NPs induced a sensitizer response in the epidermis.

5.4 Recommended Additional Research

Concerns regarding dermal exposure to nanoparticles include direct cell toxicity, accumulation in the skin, metabolism of particles into smaller components, or increased particle toxicity after ultra violet irradiation (Tsuji and others, 2006:44). Accumulation and absorption into the skin occur through any of the following pathways: between the intercellular lipid pathway in the stratum corneum, by cellular uptake, or through the hair follicle or sweat ducts (Monteiro-Riviere and Inman, 2005:1071). Figure 16 illustrates the approach used by the Biological Interaction of Nanoparticles (BIN) team at the Air Force Research Laboratory to assess the cytotoxicity and cellular interaction of

nanoparticles that have an Air Force application. The highlighted bullets represent the work completed during this study. As seen in the illustration, there is a significant amount of research needed in order to assess the biological effects of AL NPs on human skin.

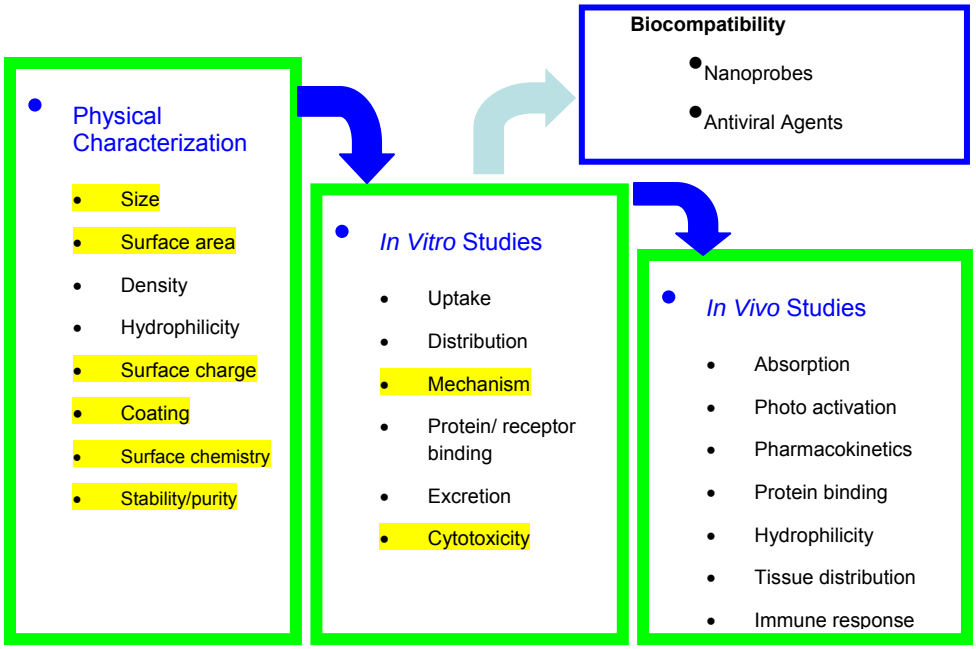

Figure 16. Biological Interaction of Nanoparticles. AFRL/RHBP, BIN Team Approach. Illustration provided by Dr. Saber Hussain. Highlights indicate research performed during this study.

5.5 Occupational Health Challenges

Proponents and skeptics of nanotechnology agree with the opinion that the full potential of nanotechnology must also address any safety, health, and environmental issues (Nel and others, 2006:622). To this end, the Nanotechnology Environmental and Health Implications (NEHI) Working Group defined five research categories to indentify and prioritize research needs, and to consolidate overlapping requirements. The five categories are: (1) instrumentation, metrology, and analytical methods; (2) nanomaterials and human health; (3) nanomaterials and the environment; (4) health and environmental

exposure assessment; and (5) risk management methods. Each of these five categories touches some aspect of the occupational setting, the potential impact that nanotechnology may have on the worker, and addresses the potential pathways of nanoparticles, from synthesis to biological system (see Figure 17).

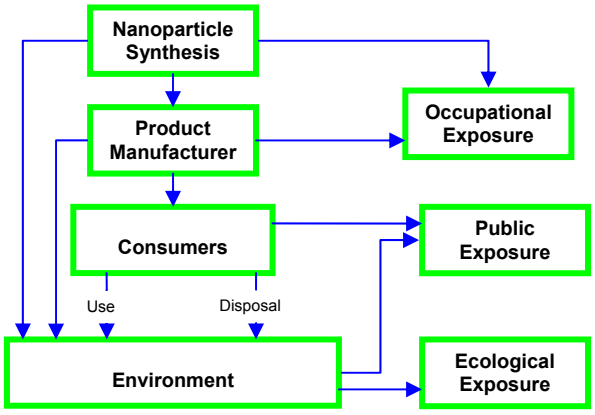

Figure 17. Potential Nanomaterial Release and Exposure.
(Adapted from Tsuji, 2006:48)

Worker exposure to nanoparticles may occur during nanoparticle synthesis, from degradation of products containing nanoparticles (bound nanoparticles), from the manufacture of nanoparticles, or the use of nanoparticles in maintenance/repair processes. "In the absence of scientific clarity about the potential health effects of occupational exposure to nanoparticles, a need exists for guidance in decision making about hazards, risks, and controls" (Schulte and Salamanca-Buentello, 2007:5). For the industrial hygienist or safety professional, the list of unanswered questions addressing the hazards of nanotechnology poses a unique challenge (see Table 11). The knowledge list in category 1 is based on the current generation of engineered nanoparticles, and existing knowledge of airborne ultrafine particles and gases. Category 2 summarizes the questions being addressed with current research. Category 3 refers to existing assessment

and control knowledge that might be ignored when assessing worker risk. Proprietary information is listed under this category because the industrial hygienist should be aware that it could be a source of information when assessing occupational health hazards. Finally, category 4 is a brief list of possible future scenarios.

Table 11. Summary of Knowledge About Nanoparticles (adapted from Schulte and Salamanca-Buentello, 2007:7)

Knowledge Awareness	Content of Knowledge
Category 1. What we know we know	Health effects of ultrafine particles, air pollution and fibers How to control ultrafine in workplace Importance of size, surface area, and surface chemistry of nanoparticles Health effects of some nanoparticles in animals Movement of some nanoparticles along the olfactory nerve in animals
Category 2. What we know we do not know	Measurement and characterization techniques Hazards of newly engineered particles Extent of translocation in body Nanoparticle interaction with workplace contaminants Importance of dermal exposure Health effects in workers Risk to workers Effectiveness of controls, medical screening, and biological monitoring Risk to worker's families
Category 3. What we do not know we know	Extensive experience available in controlling hazardous substances that may be applicable to nanoparticles (radiation, biologicals, pharmaceuticals, grain and mineral dusts) Lessons from previous "miracle" materials (asbestos) Proprietary information
Category 4. What we do not know we do not know	Unanticipated new hazards Unanticipated new controls Wrong assumptions about hazards and controls (lack of awareness)

Addressing the uncertainty of occupational risks posed by macrosized materials usually involves a single risk assessment and the implementation of a single management/control strategy. Because any of the various characteristics of a nanoparticle may pose an occupational health hazard, the industrial hygienist should consider performing a risk assessment for each type of particle, and on each characteristic of the nanoparticle. Figure 18 illustrates some of the criteria that an industrial hygienist should address when performing a nanoparticle risk assessment. Regardless of the level

of knowledge, the ultimate ethical requirement that an industrial hygienist must adhere to is to accurately portray the risk and the hazard, and to not over or understate it (Schulte and Salamanca-Buentello, 2007:8). As the knowledge and understanding of nanotechnology grows, the potential hazards and risks to workers will change over time, and may require periodic risk assessments to ensure that appropriate controls are in place.

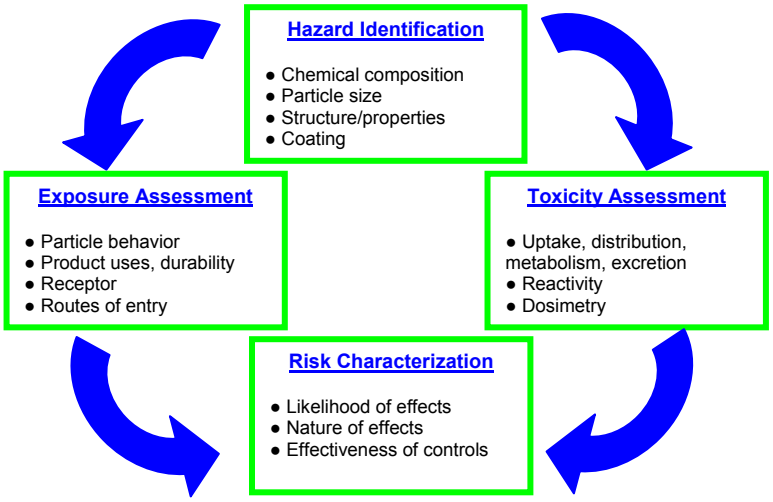

Figure 18. Risk Assessment Framework.
(Adapted from Tsuji, 2006:48)

Since the dermal health risk posed by nanoparticles, in general, and specifically AL NPs, is incomplete, care must be taken when selecting and implementing occupational skin exposure controls. Current research indicates that nanoparticles may behave in the same manner as ultrafine particles, and, in the interim, nanoparticles should be given the same level of concern (Schulte and Salamanca-Buentello, 2007:9). Although, the health hazards posed by ultrafine particles are a function of toxicity and length of exposure, and not based on particle characteristics, adopting controls used for ultrafine particles will provide workers with some level protection against nanoparticles.

5.6 Conclusion

In summary, AL NPs with the charge and surface chemistry of the particles used in this study, did not induce cell membrane leakage, reduce cell proliferation, generate ROS, or cause inflammation of keratinocytes. Based on the results of this research, AL NPs can be classified as a sensitizer agent. Since sensitization has been identified in persons exposed to aluminum in deodorant, vaccines, and toothpaste, it is likely caused by the aluminum content vs. the size of the particles. Another argument that the aluminum content is likely the cause of sensitization is supported by the fact that keratinocyte expression of the IL-8 concentrations was dependent on the concentration of the dosing stock vs. the size of the nanoparticles. Until further information is available on the biological interaction of AL NPs and human skin, care should be taken to minimize worker contact with AL NPs.

With the rapid adoption of nanotechnology and the lack of data about its health impacts, employers must accurately communicate potential health hazards and risks to their workers, and take precautionary measures to control the risks. Despite the lack of knowledge on the hazards of nanoparticles, industrial hygienists have the experience needed to perform interim risks assessments. These risk assessment can then be used to assist employers with the selection and implementation of adequate controls, and to help communicate these risks to workers in a manner that makes the risks seem reasonable and acceptable.

Appendix A: Passaging Cells

Procedure used to culture and sustain HaCaT cell line.

1. Vacuum excess liquid from cell culture flasks.
2. Wash cells with 5 mL of 1X PBS.
3. Vacuum liquid from flask.
4. Add 2.5 mL of 1 percent trypsin.
5. Incubate for 5 minutes at 37°C.
6. Add 20 mL of growth media to new cell culture flask.
7. Remove flask from incubator and add 10 mL of growth media.
8. Flush with pipette to create a single cell suspension.
9. Seed cell culture flask from step 6 with 3.5 mL of lysed cells. At this point, follow steps outline in Appendix B, Counting and Plating Cells with left over cell suspension.
10. Incubate flask at 37°C for 48 hours, until 90-100 percent confluent.

Appendix B: Counting and Dosing Cells

Procedure used to transfer an adequate number of keratinocytes to well plates.

1. After passaging (day 3), add 10 mL of growth media and the remainder of all cells from flasks to a 50 mL conical tube.

2. Pipette the solution up and down to create a single cell suspension.

3. Pipette 10 µL of the suspension on to a hemocytometer and add cover slip.

4. Place the hemocytometer under microscope and count all cells in the 4-corner grid.

5. Divide the total number of cells by 4 and then divide by 0.1 to estimate the cells/µL.

   Example: (127 cells ÷ 4) ÷ 0.1 = 318 cells per µL of cell suspension

6. Use the following equation to calculate the volume of cell suspension and cell growth media needed to seed each well.

   Example: 50,000 (cells per well) ÷ 318 cells/µL = 157 cells/well

   (96 wells/plate * 3 plates) * 0.2 mL per well * 157 cells/well

   = 9.0 mL of cell suspension needed

   (96 wells/plate * 3 plates) * 0.2 mL per well

   = 57.6 mL total volume needed

   57.6 mL – 9 mL = 48.6 mL cell growth media

7. Pipette required volumes of cell suspension and growth media into a sterile beaker. Pipette up and down to create single cell suspension.

8. Pipette the volume of the cell suspension into well plates. Use 96-well plate for assay tests and 6-well plate for morphology experiments. Incubate plates for 24 hours at 37°C.

9. After 24 hours of incubation, remove media from wells. Dose four wells with nanoparticle dosing stock and exposure media. Calculate the appropriate number of wells to act as controls (do not dose with AL NPs), add 200 µL of exposure media, and incubate plate for 24 hours at 37°C.

Appendix C: LDH Assay

Procedure used to determine if exposure to AL NPs cause keratinocyte cell membrane leakage by measuring the concentration of lactate dehydrogenase. These instructions are appropriate for the Promega, Cytotoxic-One™, Homogeneous Membrane Integrity Assay, TB306.

1. Follow Appendix B for counting, plating, and dosing cells in 96-well plate. Perform this assay experiment after 24-hour exposure of keratinocytes to nanoparticle stock.

2. Prepare LDH positive control: Add 1 μL of positive control (G181A) to 5 mL of 1X PBS. Shelf life for LDH positive control is 3 days.

3. Aliquot 50 μL of supernate from each well and transfer to a clean 96-well plate, leave 3 wells empty for positive control. Add 50 μL of LDH positive control to the 3 wells empty wells

4. Add 50 μL of LDH substrate solution to each well. To prepare LDH substrate solution, add 11 mL of assay buffer (G790B) to bottle of substrate mix (G179A). Gently, tap and slide plate from side-to-side to ensure substrate solution is well mixed with cell supernate.

5. Incubate plate, in the dark, for 10 minutes.

6. Add 25 μL of stop solution (G791A) to each well.

7. Measure fluorescence of color reaction in each well using a spectrofluorometer to excite the supernate at 560 nm and read emission at 590 nm.

8. Percent LDH leakage is compared to the blank control (zero nanoparticle). Blank control represents zero leakage. Results are calculated by $[F]_{test}/[F]_{control} \times 100$. $[F]_{test}$ is the fluorescence of test sample and $[F]_{control}$ is the fluorescence of the control sample.

Appendix D: MTS Assay

Procedure used to determine the effects of AL NPs on keratinocyte cell growth/proliferation. Living cells convert MTS (3-(4,5-dimethylthiazol-2-yl)-5-(3-carboxymethoxyphenyl)-2-(4-sulfophenyl)-2H-tetrazolium, inner salt) to formazan. The production of formazan is proportional to the number of living cells.

1. Follow Appendix B for counting, plating, and dosing cells in 96-well plate. Perform this assay experiment after 24-hour exposure of keratinocytes to nanoparticle stock. Remove exposure media and nanoparticle dosing stock from wells.

2. Wash wells 3 times with 200 μL of 1X PBS.

3. Add 100 μL exposure media to each well.

4. Add 20 μL of MTS reagent to each well.

5. Incubate at 37°C for 4 hours until the control wells change from yellow to red.

6. Use spectrophotometer to read light absorbance at 490 nm.

7. Percent MTS reduction is compared to the blank control (zero nanoparticle). Blank control represents zero reduction. Results are calculated by $[A]_{test}/[A]_{control}$ x 100. $[A]_{test}$ is the absorbance test sample and $[A]_{control}$ is the absorbance of the control sample.

Appendix E: ROS Assay

Procedure used to quantify all reactive oxygen species produced by keratinocytes undergoing oxidative stress from exposure to AL NPs.

As described in Wang H. and J.A. Joseph. "Quantifying Cellular Oxidative Stress by Dichlorofluorescein Assay Using Microplate Reader", *Free Radical Biology and Medicine*, 27(5/6): 612-616 (September 1999).

1. Follow Appendix B for counting and plating cells in 96-well plate, do not dose keratinocytes with AL NPs until after adding fluorescent probe. Use light blocking plate and seed wells for a 150K cell density. Do not perform step 9 of Appendix B.

2. Remove growth media from wells. Add 200 μL of 100 μM DCFH-DA* to each well and incubate at room temperature for 30 minutes. Keep plate out of the light.

   *Prepare 10 mM DCFH-DA (2',7'-dichlorofluorescein diacetate):
   Weigh 48 mg of DCFH-DA and add to 10 mL of DMSO (dimethly sulfoxide).
   Pipette 50 μL into 5 mL of growth media to create 100 μM DCFH-DA.

3. Remove DCFH-DA from wells.

4. Add 200 μL of AL NP suspension or positive control** to each well. Three wells for each concentration. Use media that does not contain phenol red in AL NP suspension.

   ** Prepare positive control:
   Pipette 114 uL of 30 percent H_2O_2 into 10 mL 1X PBS = 100 mM H_2O_2
   Use positive control stock and cell exposure media to prepare standard concentrations of 10 – 2000 uM.

5. Cover plate with foil and incubate at 37°C for appropriate exposure intervals up to 24 hours.

6. At appropriate time intervals (0, 1, 2, 4, 6, 24-hours) measure fluorescence of the cells in each well using a spectrofluorometer to excite the cells at 485 nm and read emission at 530 nm. ROS fold increase is calculated by $[F]_{test}/[F]_{control}$. $[F]t_{est}$ is the fluorescence of test sample and $[F]_{control}$ is the fluorescence of the control sample.

Appendix F: IL-1α Assay

Procedure used to quantify the concentration of human IL-1α expressed by keratinocytes after exposure to AL NPs.

1. Follow Appendix B for counting, plating, and dosing cells in 6-well plate.

2. Perform this assay experiment after 24-hour exposure of keratinocytes to nanoparticle stock.

3. Pipette cell supernate from each well and place in sterile, 15 mL conical tubes, one tube for each well.

4. Place 15 mL tubes in centrifuge for 15 minutes (1200 rpm) or until the nanoparticles settle to the bottom of the tube.

5. Follow instructions for Quantikine® Human IL-1α/IL-1F1 Immunoassay. See Figure 19 for a summary of the assay procedures.

6. Use absorbance data for interleukin standards to generate a Four Parameter (4-PL) Logistic Curve. Calculate concentration of test samples using nonlinear regression equation generated from the 4-PL curve.

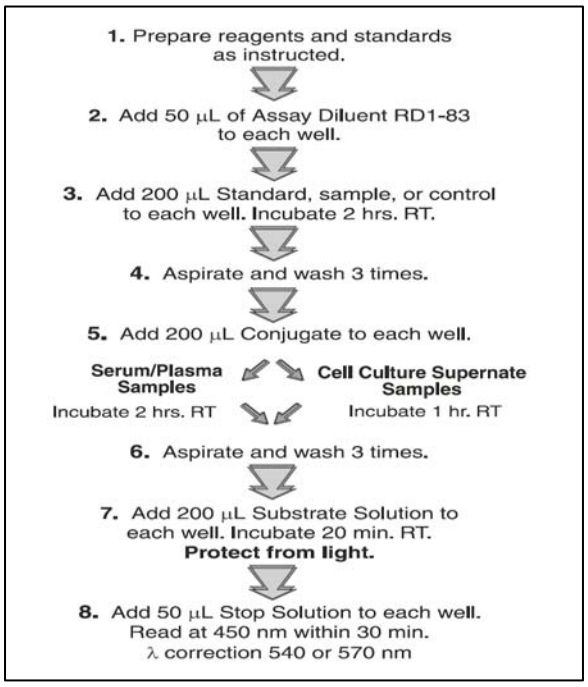

Figure 19. Summary of IL-1α Assay Procedures
Reprinted with permission from R & D Systems®, Inc.,
Quantikine® Human IL-1α/IL-1F1 Immunoassay,
Catalog DLA50 (May 2007)

Appendix G: IL-8 Assay

Procedure used to quantify the concentration of human IL-8 expressed by keratinocytes after exposure to AL NPs.

1. Follow Appendix B for counting, plating, and dosing cells in 6-well plate.

2. Perform this assay experiment after 24-hour exposure of keratinocytes to nanoparticle stock.

3. Pipette cell supernate from each well and place in sterile, 15 mL conical tubes, one tube for each well.

4. Place 15 mL tubes in centrifuge for 15 minutes (1200 rpm) or until the nanoparticles settle to the bottom of the tube.

5. Follow instructions for Quantikine® Human CXCL8/IL-8 Immunoassay. See Figure 20 for a summary of the assay procedures.

6. Use absorbance data for interleukin standards to generate a Four Parameter (4-PL) Logistic Curve. Calculate concentration of test samples using nonlinear regression equation generated from the 4-PL curve.

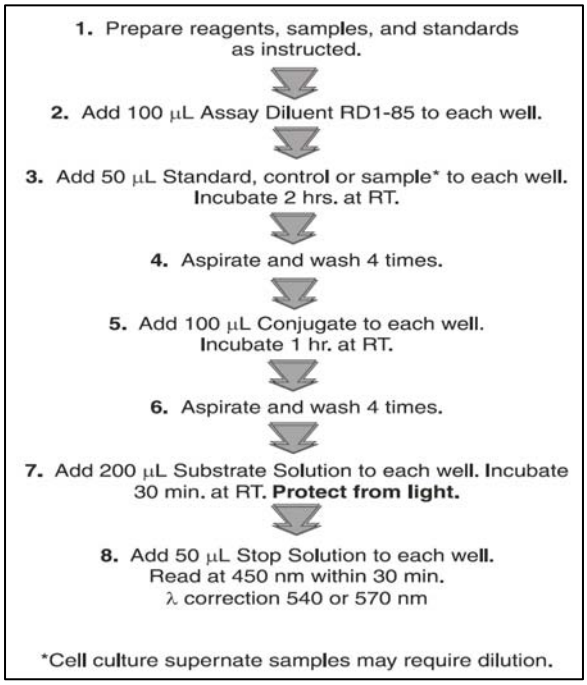

Figure 20. Summary of IL-8 Assay Procedures, Reprinted with permission from R& D Systems®, Inc., Quantikine® Human CXCL8/IL-8 Immunoassay, Catalog D8000C (September 2007)

Bibliography

3DScience. "Structure of the Skin" illustration, Wikipedia, 19 January 2007, http://en.wikipedia.org/wiki/Image:3DScience_skin_section_labeled.jpg

Ale, Iris S. and Howard I. Maibach. "Irritant Contact Dermatitis vs Allergic Contact Dermatitis" in *Dermatotoxicology, 6th Edition*. Eds. Hongbo Zhai and Howard I. Maibach. Boca Raton FL: CRC Press LLC, 2004.

Alfrey, Allen C., Arlene Hegg, and Peter Craswell. "Metabolism and Toxicity of Aluminum in Renal Failure", *The American Journal of Clinical Nutrition*, 33: 1509-1516 (July 1980).

ASTM Standard D4187-82, American Society for Testing and Materials, "Zeta Potential of Colloids in Water and Waste Water", 1985.

ATSDR, Division of Toxicology and Environmental Medicine ToxFAQs™, *Aluminum CAS # 7429-90-5*, September 2006. http://www.atsdr.cdc.gov/tfacts22.pdf

Becaria, A., A. Campbell, and S. C. Bondy. "Aluminum as a Toxicant", *Toxicology and Industrial Health*, 18: 309-320 (August 2002).

Boukamp, Petra, Rule T. Petrussevska, Dirk Breitkreutz, Jürgen Hornung, Alex Markham, and Norbert E. Fusenig. "Normal Keratinization in a Spontaneously Immortalized Aneuploid Human Keratinocyte Cell Line", *The Journal of Cell Biology*, 106: 761-771 (March 1988).

Braydich-Stolle, Laura, Saber Hussain, John J. Schlager, and Marie-Claude Hoffman. "*In Vitro* Cytotoxicity of Nanoparticles in Mammalian Germ-Line Stem Cells", *Toxicological Sciences*, 88(2): 412-419 (July 2005).

Carlin, Richard T. and Karen Swider-Lyons. "Power from the Structure Within: Application of Nanoarchitectures to Batteries and Fuel Cells", *The AMPTIAC Newsletter*, 6(1): 25-30 (Spring 2006).

Catalog #D800C: *Quantikine® Human CXCL8/IL-8 Immunoassay*, R& D Systems®, Inc., Minneapolis MN, September 2007, http://www.rndsystems.com/pdf/d8000c.pdf.

Catalog #DLA50: *Quantikine® Human IL-1α/IL-1F1 Immunoassay*, R & D Systems®, Inc., Minneapolis MN, May 2007, http://www.rndsystems.com/pdf/dla50.pdf.

Chabot-Fletcher, Marie, John Breton, John Lee, Peter Young, and Don E. Griswold. "Interleukin-8 Production Is Regulated by Protein Kinase C in Human Keratinocytes" *Journal of Investigative Dermatology*, 103(4): 509-515 (October 1994).

Coquette A., N. Berna, A. Vandenbosch, M. Rosdy, B. De Wever, and Y. Poumay. "Analysis if interleukin-1α (IL-1α) and interleukin-8 (IL-8) Expression and Release in *In Vitro* Reconstructed Human Epidermis for the Prediction of *In Vivo* Skin Irritation and/or Sensitization", *Toxicology in Vitro*, 17(3): 311-321 (June 2003).

Coquette A., N. Berna, A. Vandenbosch, M. Rosdy, and Y. Poumay. "Differential Expression and Release of Cytokines by an *In Vitro* Reconstructed Human Epidermis Following Exposure to Skin Irritant and Sensitizing Chemicals", *Toxicology in Vitro*, 13(6): 867-877 (December 1999).

Danoi, Ericka Blount. "Extraordinary Products in a Growing Market", *Black Enterprise*, 38(20): 87-91 (September 2007).

Feliciani, C., A. K. Gupta, and D. N. Saucier. "Keratinocytes and Cytokine/Growth Factors", *Critical Reviews in Oral Biology and Medicine*, 7(4): 300-318 (January 1996).

Fink, Susan L. and Brad T. Cookson. "Apoptosis, Pyroptosis, and Necrosis: Mechanistic Description of Dead and Dying Eukaryotic Cells", *Infection and Immunity*, 73(4): 1907-1916 (April 2005).

Flarend, R., T. Bin, D. Elmore, and S. L. Hem. "A Preliminary Study of the Dermal Absorption of Aluminum from Antiperspirants Using Aluminum-26", *Food and Chemical Toxicology*, 39(2): 163-168 (February 2001).

Gregus, Zoltán and Curtis D. Klaassen. "Mechanisms of Toxicity" in *Casarett & Doull's Toxicology: The Basic Science of Poisons, 6th Edition*. Ed. Curtis D. Klaassen. New York: McGraw-Hill, 2001.

Guy, Richard H., Jurji J. Hostýnek, Robert S. Hintz, and Cynthia R. Lorence. *Metals and the Skin, Topical Effects and Systemic Absorption*, New York NY: Marcel Dekker Inc., 1999.

Hoet, Peter H. M., Irene Brüske-Hohlfeld, and Oleg V Salata. "Nanoparticles – Known and Unknown Health Risks", *Journal of Nanobiotechnology,* 2 (12): 1-15 (December 2004).

Hussain, S. M., C. Carlson, L. K. Braydich-Stolle, A.M. Schrand, R.C. Murdock, A.J. Wagner, C.M. Braninshki, K.O. Yu, M.L. Shelley, D.R. Mattie, and J.J. Schlager. "Toxicity Evaluation of Nanomaterials: Technical Challenges", Unpublished. Applied Biotechnology Branch, Human Effectiveness Directorate, Air Force Research Laboratory, Wright-Patterson AFB OH.

Kabacoff, Lawrence T. "Nanoceramic Coatings Exhibit Much Higher Toughness and Wear Resistance than Conventional Coatings", *The AMPTIAC Newsletter*, 6(1): 37-42 (Spring 2006).

Kristensen, Mette S., Kirsten Paludan, Christian G. Larsen, Claus O.C. Zachariae, Bent W. Deleuran, Peter K.A. Jensen, Poul Jorhensen, and Kristian Thestrup-Pedersen. "Quantitative Determination of IL-1α-Induced IL-8 mRNA Levels in Cultured Human Keratinocytes, Dermal Fibroblasts, Endothelial Cells, and Monocytes", *Journal of Investigative Dermatology*, 97(3): 506 510 (September 1991).

Lines, M. G. "Nanomaterial for Practical Functional Uses", *Journal of Alloys and Compounds*, 449(1-2): 242-245 (January 2008).

Luca, Costantino, Francesca Gandolfi, Giovanni Tosi, Francesco Rivasi, Maria Angela Vandelli, and Flavio Forni. "Peptide-Derivatized Biodegradable Nanoparticles Able to Cross the Blood–Brain Barrier", *Journal of Controlled Release*, 108: 84-96 (July 2005).

Maney, Kevin. "Nanotech Could Put a New Spin on Sports", *USA Today* (November 17, 2004).

Marzulli, Francis N. and Howard I. Maibach. "Allergic Contact Dermatitis" in *Dermatotoxicology, 6th Edition*. Eds. Hongbo Zhai and Howard I. Maibach. Boca Raton FL: CRC Press LLC, 2004.

Mattie, D. R. Applied Biotechnology Branch, Air Force Research Laboratory, Human Effectiveness Directorate, Wright-Patterson AFB OH. Personal Interview. 12 Feb 2007.

Maysinger, Dusica, Maik Behrendt, and Ewa Przybytkowski. "Death by Nanoparticles?", *NanoPharmaceuticals Online Journal*, 1: 1-21 (October 2006).

Maynard, Andrew D. "Safe Handling of Nanotechnology", *Nature*, 444(16): 267-269 (November 2006).

Monteiro-Riviere, Nancy A. and Alfred O. Inman. "Challenges for Assessing Carbon Nanomaterial Toxicity to the Skin", *Carbon*, 44(6): 1070-1078 (May 2006).

McDougal, James N., Daniel L. Pollard, Wade Weisman, Carol M. Garrett, and Thomas E. Miller. "Assessment of Skin Absorption and Penetration of JP-8 Jet Fuel and Its Components", *Toxicological Sciences*, 55: 247-255 (January 2000).

Miziolek, Andrzej W. "Nanoenergetics: An Emerging Technology Area of National Importance", *The AMPTIAC Newsletter*, 6(1): 43-48 (Spring 2006).

National Science and Technology Council, Committee on Technology, Subcommittee on Nanoscale Science, Engineering, and Technology. *The National Nanotechnology Initiative, Strategic Plan*, December 2007.

National Science and Technology Council, Committee on Technology, Subcommittee on Nanoscale Science, Engineering, and Technology. *Prioritization of Environmental, Health, Safety Research Needs for Engineered Nanoscale Materials*, August 2007.

Nel, Andre, Tian Xia, Lutz Madler, and Ning Li. "Toxic Potential of Materials at the Nanolevel", *Science*, 311: 622-627 (February 2006).

Oberdorster, Gunter, Eva Oberdorster, and Jan Oberdorster. "Nanotoxicology: An Emerging Discipline Evolving from Studies of Ultrafine Particles", *Environmental Health Perspectives*, 113(7): 823-839 (July 2005).

Office of Science and Technology Policy, Executive Office of the President, National Nanotechnology Initiative, *Research and Development Funding in the President's 2006 Budget*, http://www.nano.gov/html/facts/faqs.html.

Palaszewski, Bryan, John Jurns, Kevin Breisacher, and Kin Kearns. National Aeronautics and Space Administration, *Metallized Gelled Propellants Combustion Experiments in a Pulse Detonation Engine*, NASA/TM-2006-214119, October 2006.

Patten, Mildred L. *Understanding Research Methods, Fifth Edition*, Glendale CA, Pyrczak Publishing, 2005

Paul, William E. *Fundamental Immunology (Second Edition)*. New York: Raven Press, 1989.

"Powders: Unique Nanoparticles for Advanced Applications", NovaCentrix™ Corp, Austin TX, 24 January 2008, http://www.nanoscale.com/products/powders.php.

Rooney, Aubrey D., Rochelle L. Jones, David R. Mattie, John J. Schlager, and Saber M. Hussain. United States Air Force Research Laboratory, *In Vitro Toxicity of Nanoparticles in Mouse Keratinocytes and Endothelial Cells*, AFRL-HE-WP-TR-2005-0091, June 2004.

Saba, Mark, MA. "Structure of Epidermis" illustration, Yale ITS Media Technology Services, January 2007, http://www.yale.edu/its/media/art/portfolio_powerpoint.

Sass, Jennifer. "Nanotechnology's Invisible Threat – Small Science, Big Consequences", *National Resources Defense Council Issue Paper*, May 2007.

Schrand, Amanda. Applied Biotechnology Branch, Air Force Research Laboratory, Human Effectiveness Directorate, Wright-Patterson AFB OH. Personal Interview. 30 November 2007.

Schulte Paul A. and Fabio Salamanca-Buentello, "Ethical and Scientific Issues of Nanotechnology in the Workplace", *Environmental Health Perspectives*, 15(11): 5-12 (January 2007).

Technical Bulletin 169: *CellTiter 96® AQ_{ueous} Non-Radioactive Cell Proliferation Assay*, Promega Corporation., Madison WI, revised April 2005, http://www.promega.com/tbs/tb169/tb169.pdf.

Technical Bulletin 306: *Cytotoxic-One™ Homogeneous Membrane Integrity Assay*, Promega Corporation., Madison WI, revised May 2007, http://www.promega.com/tbs/tb306/tb306.pdf.

Toimela, Tarja, Hanna Mäonpää, Marika Mannerström, and Hanna Tähti. "Development of an *In Vitro* Blood-Brain Barrier Model-Cytotoxicity of Mercury and Aluminum", *Toxicology and Applied Pharmacology*, 195: 73-82 (July 2000).

Tsuji, Joyce S., Andrew D. Maynard, Paul C. Howard, John T. James, Chiu-wing Lam, David B. Warheit, and Annette B. Santamaria. "Research Strategies for Safety Evaluation of Nanomaterials, Part IV: Risk Assessment of Nanoparticles", *Toxicological Sciences*, 89(1): 42-50 (January 2006).

U.S. Department of Labor, Bureau of Labor Statistics, Injuries, Illnesses, and Fatalities, as of January 2007, http://data.bls.gov/cgi-bin/surveymost.

Veien, Niels K., Thais Hattel, and Grete Laurberg. "Systemically Aggravated Contact Dermatitis Caused by Aluminum in Toothpaste", *Contact Dermatitis*, 28: 199 – 200 (March 1993).

Wagner, Andrew J. *In Vitro Toxicity of Aluminum Nanoparticles in Rat Alveolar Macrophages*, MS Thesis, AFIT/GES/ENV/06M-06. School of Engineering and Management, Air Force Institute of Technology (AU), Wright-Patterson AFB OH, March 2006 (ADA446266).

Wagner, Andrew J., Charles A. Bleckmann, Richard C. Murdock, Amanda M. Schrand, John J. Schlager, and Saber M. Hussain. "Cellular Interaction of Different Forms of Aluminum Nanoparticles in Rat Alveolar Macrophages", *The Journal of Physical Chemistry B*, 111: 7353-7359 (June 2007).

Wang H. and J. A. Joseph. "Quantifying Cellular Oxidative Stress by Dichlorofluorescein Assay Using Microplate Reader", *Free Radical Biology and Medicine*, 27(5/6): 612-616 (September 1999).

Weltfriend, Sara, Michal Ramon, and Howard I. Maibach. "Irritant Dermatitis" in *Dermatotoxicology, 6th Edition*. Eds. Hongbo Zhai and Howard I. Maibach. Boca Raton FL: CRC Press LLC, 2004.

Wyllie, Andrew H. "Cell Death" in *Apoptosis, Cell Death, and Cell Proliferation, 3rd Edition*. Eds. Hans-Jürgen Rode, Doris Eisel, and Inge Frost. Roche Applied Science, Indianapolis IN, February 2008.

Xia, Tian, Michael Kovochich, Jonathan Brant, Matt Hotze, Joan Sempf, Terry Oberley, Constantinos Sioutas, Joanne I. Yeh, Mark R. Wiesner, and Andre E. Nel. "Comparison of the Abilities of Ambient and Manufactured Nanoparticles to Induce Cellular Toxicity According to an Oxidative Stress Paradigm", *Nano Letters*, 6(8): 794-1807 (July 2006).

Zeta-Meter Inc. *Zeta Potential: A Complete Course in 5 Minutes*, as of 30 January 2008, http://www.zeta-meter.com/5min.pdf.

Vita

Major Stephanie McCormack-Brown graduated from Norwich University, Vermont in May of 1991 with a Bachelor of Science in Environmental Engineering Technology and a minor in Chemistry. In August 2003, Major Brown completed a Masters of Science degree in General Administration from Central Michigan University. Major Brown was commissioned into the Air Force in May 1991. Since January 1992, she has been assigned to a variety of Bioenvironmental Engineering positions at Robins AFB GA, Hickam AFB HI, and Grand Fork AFB ND. In 2005, Major Brown deployed to Al Udeid AB, Qatar in support of Operation Iraqi Freedom and Operation Enduring Freedom. Major Brown attended AFIT as a student in the first Industrial Hygiene graduate program. Upon graduation, she will be assigned to the Air Force Institute of Operational Health, Brooks City Base TX. Major Brown is a Certified Industrial Hygienist, American Board of Industrial Hygiene.

REPORT DOCUMENTATION PAGE

Form Approved
OMB No. 074-0188

1. REPORT DATE *(DD-MM-YYYY)*	**2. REPORT TYPE**	**3. DATES COVERED** *(From – To)*
27-03-2008	Master's Thesis	Jun 2007 – Mar 2008

4. TITLE AND SUBTITLE

In Vitro Toxicity Of Aluminum Nanoparticles In Human Keratinocytes

5a. CONTRACT NUMBER

5b. GRANT NUMBER

5c. PROGRAM ELEMENT NUMBER

6. AUTHOR(S)

McCormack-Brown, Stephanie, Major, USAF, BSC

5d. PROJECT NUMBER

5e. TASK NUMBER

5f. WORK UNIT NUMBER

7. PERFORMING ORGANIZATION NAMES(S) AND ADDRESS(S)
Air Force Institute of Technology
Graduate School of Engineering and Management (AFIT/ENV)
2950 Hobson Way
WPAFB OH 45433-7765

8. PERFORMING ORGANIZATION REPORT NUMBER

AFIT/GIH/ENV/08-M01

9. SPONSORING/MONITORING AGENCY NAME(S) AND ADDRESS(ES)
Hussain, Dr. Saber, M. AFRL/RHPB
Air Force Research Laboratory
WPAFB, Bldg 837, Area B, 2729 R St.
WPAFB OH 45433-7765
Tel: 937-904-7765

10. SPONSOR/MONITOR'S ACRONYM(S)

11. SPONSOR/MONITOR'S REPORT NUMBER(S)

12. DISTRIBUTION/AVAILABILITY STATEMENT

APPROVED FOR PUBLIC RELEASE; DISTRIBUTION UNLIMITED.

13. SUPPLEMENTARY NOTES

14. ABSTRACT

Nanotechnology promises to be the defining technology of the 21st century. At an annual investment of $1B, it provides significant contributions to manufacturing, medicine, energy conservation, and the environment. Nanoparticles are structures with at least one dimension in the 1 to 100 nanometer (nm) range. DoD and US Air Force interest in aluminum nanoparticles (AL NPs) stems from its ability to enhance combustion jet fuel, thus increasing fuel efficiency. The addition of AL NPs to JP-8 may pose a unique dermal hazard to aircraft maintenance workers. There is no published data on AL NP toxicity effects on human skin. This research used *in vitro* techniques to determine the cytotoxicity of AL NPs, sized 50, 80, and 120 nm, on human keratinocytes. AL NPs at concentrations 10 – 10,000 μg/mL and 24-hour exposure did not have a negative effect on cell viability, as assessed by membrane leakage, metabolic function, and reactive oxygen species generation. Keratinocyte expression of proinflammatory interleukins-1α and -8 was quantified to determine if AL NPs induced precursor cytokines for irritant contact or sensitizer response dermatitis. After 24-hour exposure to AL NPs, keratinocytes expressed significant concentrations of IL-8, 24 – 100 times greater than IL-1α, indicating that AL NPs may induce sensitizer response dermatitis.

15. SUBJECT TERMS
Nanotechnology, Nanomaterials, Nanoparticles, Aluminum, Keratinocytes, In Vitro, Interleukin-1α, Interleukin-8

16. SECURITY CLASSIFICATION OF:			**17. LIMITATION OF ABSTRACT**	**18. NUMBER OF PAGES**	**19a. NAME OF RESPONSIBLE PERSON**
REPORT	**ABSTRACT**	**c. THIS PAGE**			JEREMY M. SLAGLEY, Maj, USAF, BSC, PhD, CIH
U	**U**	**U**	**UU**	90	**19b. TELEPHONE NUMBER** *(Include area code)* (937) 255-3636, ext 4511; email: Jeremy.Slagley@afit.edu